water

MDPI

Article

Projections on the Spatiotemporal Bioclimatic Change over the Phytogeographical Regions of Greece by the Emberger Index

Ioannis Charalampopoulos [1,*], Fotoula Droulia [1], Ioannis P. Kokkoris [2] and Panayotis Dimopoulos [3]

[1] Laboratory of General and Agricultural Meteorology, Department of Crop Science, Agricultural University of Athens, 11855 Athens, Greece; fdroulia@aua.gr
[2] Department of Sustainable Agriculture, University of Patras, 2 G. Seferi St., 30131 Agrinio, Greece; ipkokkoris@upatras.gr
[3] Laboratory of Botany, Department of Biology, University of Patras, 26504 Patras, Greece; pdimopoulos@upatras.gr
* Correspondence: icharalamp@aua.gr; Tel.: +30-210-529-4234

Abstract: Unquestionably, the rapidly changing climate and, therefore, alterations in the associated bioclimate, constitute an alarming reality with implications for daily practice and natural capital management. This research displays the present and projected bioclimate evolution over Greece's phytogeographical regions. For this purpose, ultrahigh-resolution computation results on the spatial distribution of the Emberger index's Q2 classes of bioclimatic characterization are analyzed and illustrated for the first time. The assessments are performed over the reference period (1970–2000) and two future time frames (2021–2040; 2041–2060) under the RCP4.5 and RCP8.5 emission scenarios. By 2060 and under the extreme RCP8.5, intense xerothermic trends are demonstrated owing to the resulting significant spatial evolution mainly of the Arid–Hot, Semi-Arid–Very Hot, Semi-Arid–Hot, and Semi-Arid–Temperate Q2 classes, respectively, over the phytogeographical regions of Kiklades (up to 29% occupation), Kriti and Karpathos (up to 30%), West Aegean Islands (up to 26%), North East (up to 56%), and North Central (up to 31%). The RCP8.5 long-term period exhibits the strongest impacts over approximately the right half of the Greek territory, with the bioclimate appearing more dry–thermal in the future. In conclusion, the Emberger index provides an in-depth view of the Greek area's bioclimatic regime and the potential alterations due to climate change per phytogeographical region.

Keywords: aridisation; bioclimate classification; climate change; climate projections; natural capital management; southern Europe

Citation: Charalampopoulos, I.; Droulia, F.; Kokkoris, I.P.; Dimopoulos, P. Projections on the Spatiotemporal Bioclimatic Change over the Phytogeographical Regions of Greece by the Emberger Index. *Water* **2024**, *16*, 2070. https://doi.org/10.3390/w16142070

Academic Editors: Dariusz Wrzesiński and Leszek Sobkowiak

Received: 30 June 2024
Revised: 19 July 2024
Accepted: 20 July 2024
Published: 22 July 2024

1. Introduction

There is global scientific consensus on the anthropogenic phenomenon of climate change (CC) [1] and the related altered bioclimate by focusing on its vital impacts on humans [2,3], fauna [4–6], flora [7–9], natural resources, ecosystem–climate services, and management policies [10–13].

The Greek Peninsula in southeastern Europe appears as a future climatically threatened territory due to its rapidly changing bioclimatic conditions [14–17]. Projections on the country's changing climate reveal significant warming trends under the RCP8.5, with a near-surface temperature average rise of 4.3 °C by the end of the 21st century and, therefore, a significant increase in the annual number of hot days and tropical nights, night frosts, continuous dry spell days, and length of the growing season and a decrease in frost days. The reduction of precipitation by 16% and an increase in the annual number of consecutive dry days by 30% (15.4 days) pinpoint a future drier environmental evolution [18,19].

Furthermore, directly linked to CC, present and future extreme weather events appear modified in their frequency and intensity, e.g., an increase in extreme wind speeds [20],

more frequent flash floods and drought episodes [21–23], more often, more extreme, and longer heatwaves [24,25], and a lengthened hot extremes season [26].

Predictions on Greece's future climatic parameters' evolution conjointly with its present more xerothermic climatic footprint may justify its increasing vulnerability to CC capable of forming significant impacts on its extensive natural vegetation and highly heterogeneous agricultural ecosystems [8,27,28].

The present and projected impacts of CC on the Greek natural ecosystems involve increased wildfire and flood risks [29,30], altered fire behavior in natural landscapes [31], increase in high fire danger days [32], reduction in water availability [33], declining tree growth and productivity [34,35], dieback of tree species [36], higher extinction risk of the endemic flora [37–39], reduction in habitat-suitable areas [37,40], elevational and altitudinal shifts of dominant species, changes in forest cover [41], occurrence and spread of alien plant taxa [42], and loss of biodiversity [43].

As for the agricultural areas, respective impacts include alterations of frost agroclimatic indicators, increase in the growing season duration [44], crop yield and product quality reduction [45,46], agricultural soil losses [47], degradation of surface and groundwater resources, declining of water availability [48], crop phenology modifications [49], changes in area suitability for cultivation [50], impacts on crops' adaptive capacity [51], declining variety suitability [15], cultivations' expansion to higher altitudes and northern areas, increased frequency of crops' vulnerability (elevated heat injuries) [44,52], and rural areas' negative socio-economic evolution [53].

A thorough understanding and better capture of the phenomenon of bioclimatic change is justifiably demonstrated by the very common utilization of bioclimatic indices (mathematical formulas based on fundamental climatic parameters such as temperature and precipitation) as tools for the climate's characterization in various surveys of different scientific fields (e.g., climatology, bioclimatology, forestry, agricultural surveys, investigations on climate/bioclimate change) [15,54–70].

Temperature and precipitation are decisive climatic inputs for the exploration of CC, but the utilization of bioclimatic indices allows a more thorough understanding and better capture of the phenomenon's dimension in bioclimatic terms [71]. By exploiting the indices' values, the assessment of the effects of climate on vegetation and the environment's correlation with the predominating vegetation types is more feasible [72,73].

Based on fundamental climatic parameters (temperature, precipitation, and evaporation), the Emberger index (IEMB), commonly termed the pluviothermic quotient (Q), classifies the bioclimate zones in the Mediterranean area according to a scheme extending from the "Per-Humid" to "Per-Arid" characterization (or bioclimatic type, bioclimatic category). For the index's estimation, the temperature is represented, on an annual basis, by the average value of the maximum temperatures of the hottest month (M) and the average value of the minimum temperatures of the coldest month (m), given that vegetation development is strictly associated with these thermal limits. The precipitation (P) is expressed by its annual values, and evaporation is indirectly represented by (M—m), considering the parameter's common increase with the latter difference [54,73,74]. Concomitantly, for the phytoclimatic classification in bioclimatic subtypes (or Q2 classes), Emberger also utilized a simplified algorithm on the basis of the minimum winter temperature (m) extending from the "Very Hot" to the "Very Cold" temperature characterization [74,75]. As such, the phytoclimatic conditions' mapping is conducted through the combination of the characterizations of the bioclimatic types as obtained from the estimates of the Q values and the temperature conditions corresponding to the estimates of the m values, which results in the Q2 bioclimatic subtypes (e.g., a Q2 subtype described as "sub-humid with mild winter").

In Europe, the IEMB has been applied for the classification of the bioclimate [76,77], for investigations on the vegetation's dissemination [75,78], for surveys on the preservation (conservation, restoration, habitat suitability) of landscapes [10,63,73,79–82], and for research on the risk of desertification [10] and on changes of the bioclimatic regime [83,84].

For Greece, in particular, very limited investigations on the changes in the bioclimate have been conducted based on applications of the IEMB. Up to the present, researchers have conducted bioclimatic classifications at a very local scale involving surveys on fires and wildfire risk assessment [85–87], the bioclimatic classification of natural vegetation environments [88], reforestation potential, restoration and conservation of natural landscapes [10,88–91], plant diversity [92–95], land cover change [96], and environmental monitoring and management of water resources and water quality parameters [97,98]. The IEMB has also been applied in investigations concerning the effects of climatic factors on the fuel complex characteristics of the pine forests and on the fire activity patterns in natural vegetation formations in Greece [31,87].

Within the changing climate's research framework, the overview of previous investigations demonstrates the very limited applications of the IEMB as a tool for bioclimatic classification (mostly conducted at the local scale) and for predictions on the future of Greece's bioclimatic regime under the influence of CC.

The originality of the current research lies in the high-resolution computation (approximately 300 m) of the Emberger index's Q1 and Q2 classes of bioclimatic characterization, which are analyzed and illustrated for the first time in order to capture the present bioclimatic regime and its future evolution in a particularly extensive area represented by the entire country of Greece. This mapping material, along with the spatial statistics per phytogeographical region, could be a reference dataset for ecological, agricultural, and natural conservation applications and research.

The more detailed outcomes on the country's bioclimatic alteration drawn from this study might serve as an exhortation to implement advanced technologies for their successful preservation under the future status of an altered climate. Additionally, results for the phytogeographical regions of Greece [99] will support decision-making for targeted future research and resource allocation to enhance conservation management for habitats and species (in natural and anthropogenic, human-induced, cultural ecosystems) found in these areas.

2. Materials and Methods

2.1. Study Area

The Greek Peninsula, situated at the heart of the Mediterranean, covers a total area of 131,957 km^2 which occupies the southernmost expansion of the Balkans. The mainland represents 80% of the land area, while a vast number of approximately 3000 islands constitute the residual 20%. Lowland areas, particularly along its extensive coastline, characterize almost a quarter of the country's surface. Natural areas (rugged mountains, forests, and lakes) dominate the Greek mainland landscape, while agricultural areas appear to be less expanded.

Vast forested mountain formations (Rhodope Mountains) stretch along the Greece–Bulgaria border, extend from the Greece–Albania border to the Corinthian Gulf (Pindos Mountain range), continue in the Peloponnese geographical area (Teygetos Mountain range), and reappear in Crete (Dikti and White Mountains or Lefka Ori and the Idi Mountain range). These mountain ranges encircle fertile agricultural lands across mainland Greece (e.g., Thessaloniki Plain, Thessaly Plain, northern and western Peloponnese plains, and central Crete). A great number of the islands also demonstrate natural vegetation of incomparable specificity and variability. Therefore, it can be seen that given its natural geography and position, Greece is governed by considerable climate variation.

Greece is one of the most diverse countries in terms of flora species, hosting 6811 taxa, including 1144 Greek endemics and 1553 range-restricted [100–103], distributed among 13 well-distinguished phytogeographical regions (Strid and Tan 1997). The 13 phytogeographical regions of Greece (Figure 1) separate the Greek territory in the parts of Peloponnisos (Pe), North Central (NC), East Aegean Islands (EAe), Ionian Islands (IoI), East Central (EC), Kriti and Karpathos (KK), North Aegean Islands (NAe), Kiklades (KiK), West Aegean Islands (WAe), North East (NE), Southern Pindos (SPi), Sterea Ellas (StE), and

Northern Pindos (NPi), according to Strid and Tan [99]. The species found in each region renders its particular characteristics; in Table 1, the number of total species, endemics, and range-restricted species for each region are presented.

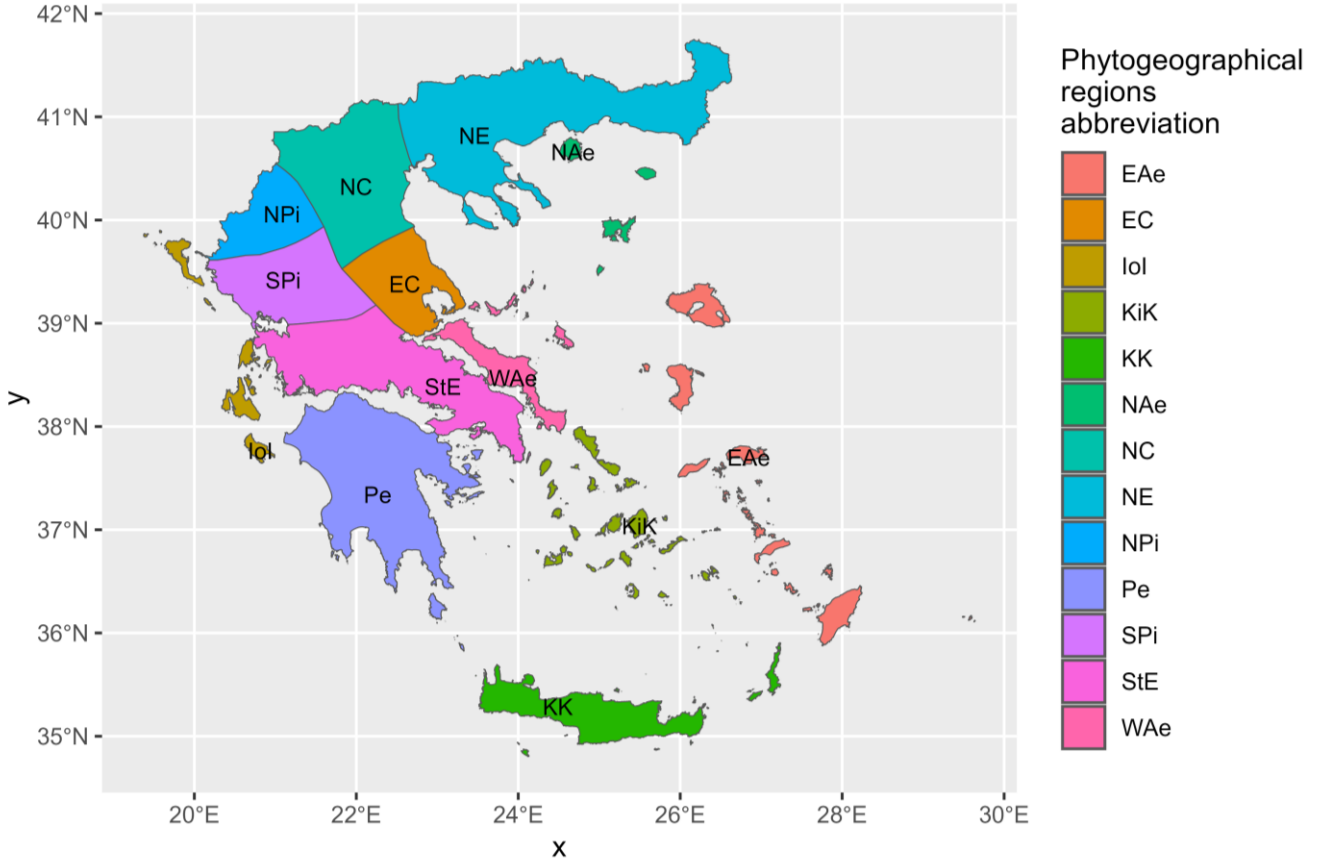

Figure 1. The phytogeographical regions of Greece as defined by Strid and Tan (1997) [46]. Peloponnisos (Pe), North Central (NC), East Aegean Islands (EAe), Ionian Islands (IoI), East Central (EC), Kriti and Karpathos (KK), North Aegean Islands (NAe), Kiklades (KiK), West Aegean Islands (WAe), North East (NE), Southern Pindos (SPi), Sterea Ellas (StE), and Northern Pindos (NPi).

Table 1. Distribution of species and sub-species (total, endemic, range-restricted) in the 13 phytogeographical regions of Greece [47].

Number	NE	NC	StE	Pe	SPi	NPi	EAe	EC	KK	WAe	NAe	IoI	Kik
Species and subspecies (total)	4440	4215	4169	4046	3502	3456	3087	2685	2679	2658	2558	2489	2206
Endemics	166	203	399	522	156	150	182	104	426	226	71	94	191
Range-restricted	414	468	519	577	301	355	292	171	423	250	99	113	197

2.2. Data and Methods

The WorldClim dataset [104], which has been used for various research topics, including ecology and agriculture from a climatic point of view [105–112], is the atmospheric dataset source for this study. More specifically, for future projections, we use the Met Office Hadley Centre HadGEM3-GC31-LL model results. From the initial resolution of ~1 km, we downscaled statistically (utilizing altitude, latitude, and Euclidean distance from the shoreline) the temperature parameters to ~250 m resolution with the SpatialEco [113] R language package. The precipitation data was resampled via the bilinear method to the same resolution. For the calculations and the mapping, the Tidyverse [114] package, especially dplyr [115] and gglot2 [116], along with the terra [117] geospatial R package, were used (Figure 2).

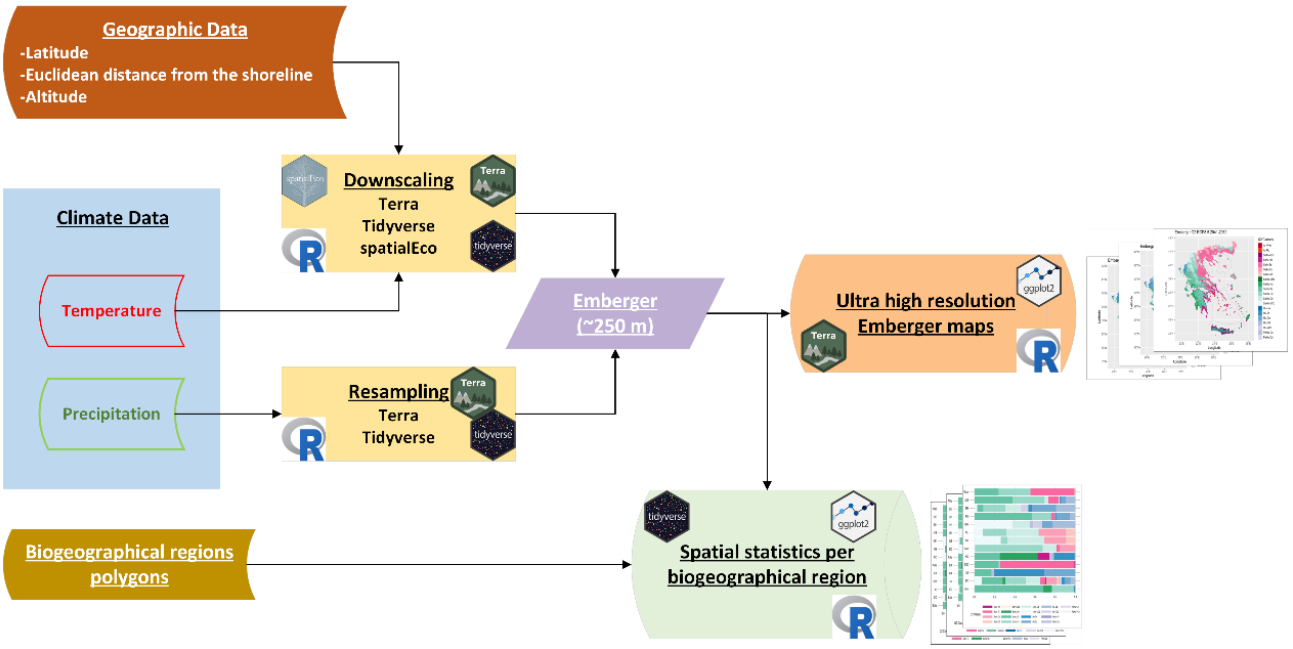

Figure 2. The performed analysis process.

The variability of the IEMB is studied over the reference period (Ref: 1970–2000) and two future time periods (p1: 2021–2040; p2: 2041–2060), computed at a high resolution of approximately 300 m under the RCP4.5 and RCP8.5 emission scenarios. The short-term and long-term bioclimatic change trends are targeted by approaching the main differences between the present and the future bioclimate regime.

The metric exploited for the evaluation of the bioclimate is the Emberger index, frequently characterized as the aridity of the bioclimate index. It is easy to apply, and it can be distinguished between two different levels. The first refers to the pluviothermic quotient (pluvio = rainfall):

$$Q1 = \frac{2000 \times P}{M^2 - m^2} \quad (1)$$

where

P is the annual precipitation,

M is the maximum air temperature of the hottest month (in K),

m is the minimum air temperature of the coldest month (in K).

According to the value of the Q1 quotient, the bioclimate can be characterized as presented in Table 2.

Table 2. Emberger Q1 classification and the related bioclimatic characterization.

Emberger Q1 Class	Bioclimatic Characterization
$Q1 > 170$	Per-Humid (PeHu)
$120 < Q1 \leq 170$	Humid (Hu)
$65 < Q1 \leq 120$	Sub-Humid (SuHu)
$30 < Q1 \leq 65$	Semi-Arid (SeAr)
$17 < Q1 \leq 30$	Arid (Ar)
$0 < Q1 \leq 17$	Per-Arid (PeAr)

The next level of the Emberger index combines the Q1 with the mean minimum air temperature of the coldest month, as shown in Table 3 and Figure 3.

Table 3. The m (mean minimum temperature of the coldest month) classification and the related characterization.

Mean Minimum Temperature of the Coldest Month (m) in °C	Temperature Characterization
m > 10 °C	Very Hot (VHo)
7 °C < m ≤ 10 °C	Hot (Ho)
3 °C < m ≤ 7 °C	Temperate (Te)
0 °C < m ≤ 3 °C	Cool (Co)
−3 °C < m ≤ 0 °C	Cold (Cd)
m ≤ −3 °C	Very Cold (VC)

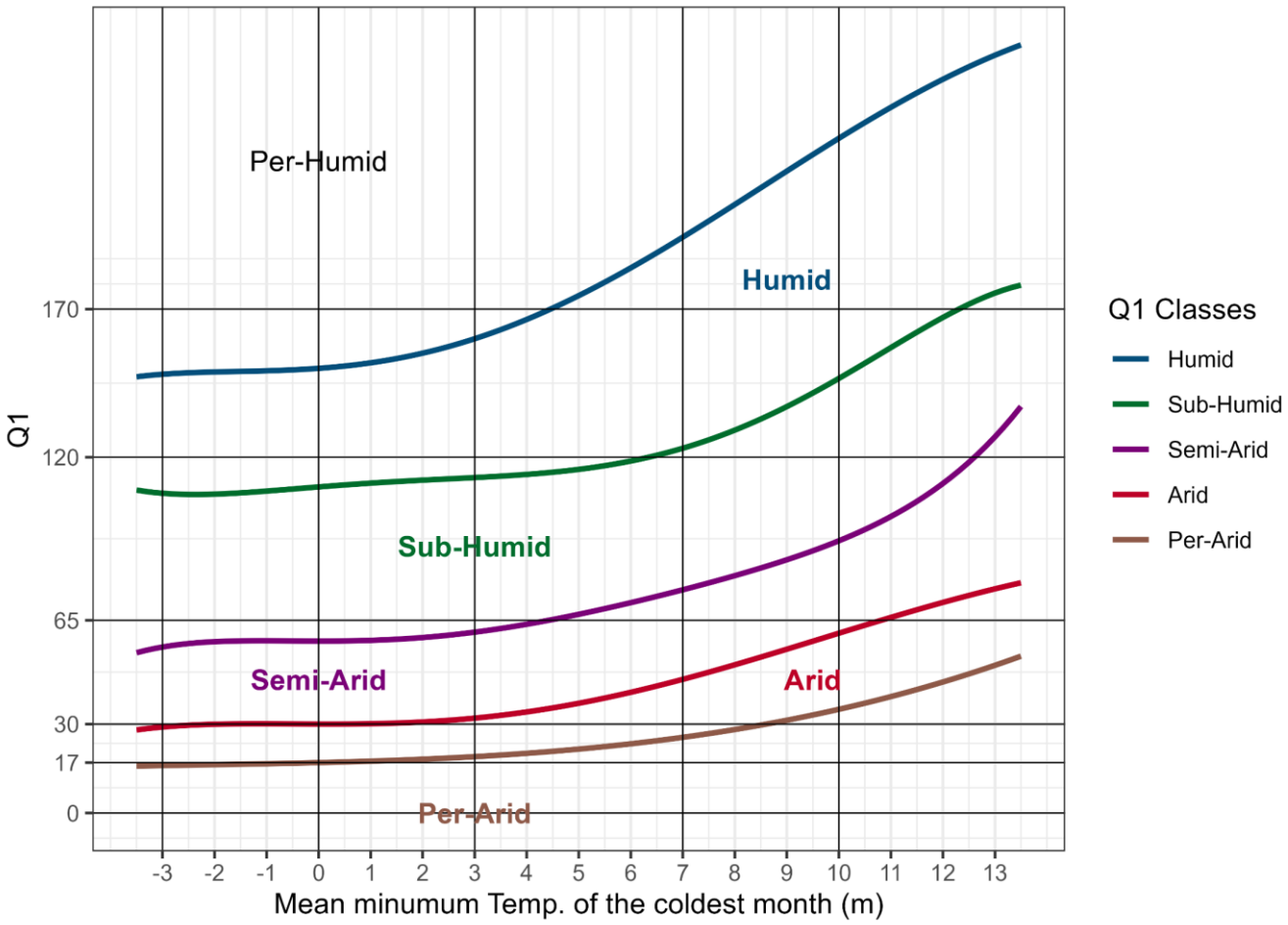

Figure 3. The Emberger climatogram encompasses the combinations of the Q1 values with the m values (mean minimum values of the coldest month).

The final characterization of the Q2 is the combination of the Q1 and the m, as displayed in Table 4. For example, when calculating the Q1 as 4 and the m as 5, the Q2 classification is characterized by the 'Per-Arid Temperate (PeAr-Te)' class.

Table 4. The Q2 classes and their abbreviations *.

	Very Hot (VHo) m > 10	**Hot (Ho) 7 < m ≤ 10**	**Temperate (Te) 3 < m ≤ 7**	**Cool (Co) 0 < m ≤ 3**	**Cold (Cd) −3 < m ≤ 0**	**Very Cold (VCd) m ≤ −3**
Per-Arid (PeAr) 0 < Q1 ≤ 17	PeAr-VHo	PeAr-Ho	PeAr-Te	PeAr-Co	PeAr-Cd	PeAr-VCd
Arid (Ar) 17 < Q1 ≤ 30	Ar-VHo	Ar-Ho	Ar-Te	Ar-Co	Ar-Cd	Ar-VCd
Semi-Arid (SeAr) 30 < Q1 ≤ 65	SeAr-VHo	SeAr-Ho	SeAr-Te	SeAr-Co	SeAr-Cd	SeAr-VCd
Sub-Humid (SuHu) 65 < Q1 ≤ 120	SuHu-VHo	SuHu-Ho	SuHu-Te	SuHu-Co	SuHu-Cd	SuHu-VCd
Humid (Hu) 120 < Q1 ≤ 170	Hu-VHo	Hu-Ho	Hu-Te	Hu-Co	Hu-Cd	Hu-VCd
Per-Humid (PeHu) 170 < Q	PeHu-VHo	PeHu-Ho	PeHu-Te	PeHu-Co	PeHu-Cd	PeHu-VCd

Note: * The background colors are the same as the Q2 classes inside maps.

3. Results and Discussion

3.1. Reference Period 1970–2000

For the reference period (1970–2000) (henceforth Ref), the presented pluviothermic quotient Q1 map's classification (Figure S1) demonstrates the Emberger's main bioclimate types' characterization by four classes (PeHu, Hu, SuHu, and SeAr), reflecting a transition toward drier conditions from the west to the east of the country. The resulting percentage area estimations of the Q1 classes' % coverage per phytogeographical region reveal the predominance of the SuHu class over the East Aegean Islands (EAe) (approximately 99%), followed mainly by Peloponnisos (Pe) (88%), Sterea Ellas (StE) (84%), Kriti and Karpathos (KK) (75%), Southern Pindos (SPi) (70%), Northern Pindos (NPi) (64%), and the North Central (NC) (51%) (Figure S2, Table S1).

According to the presented map's classification (Figure 4), all four Q1 classes are combined with temperature conditions ranging from the Te to the VCd characterization (the additional designation Ho appears only for the SuHu and SeAr types). These combinations result in a great number of bioclimatic sub-categories (18 in total).

At this point, it must be underlined that the Q2 classes' presentation in the legends but not in the spatial distribution maps (e.g., Figure 4) and percentage (%) relative surface per geographical zone charts (e.g., Figure 5) is attributed to the resulting classes' very limited (%) coverage values.

Overall, the resulting Q2 classes' relative % coverage per phytogeographical region (Figure 4 and Table S6) shows dominant distributions among the SeAr-Te (74% over Kiklades (KiK) and 44% for the West Aegean Islands (WAe)), the SuHu-Te (68% for EAe and 57% for Pe), the SuHu-Co (67% for the North Aegean Islands (NAe)) and the SuHu-Cd (36% over NC). The more humid Hu category also appears, mainly falling within the temperature conditions of Te (50% in the Ionian Islands (IoI)), Co (31% in IoI), and Cd (22% in NPi and 19% in SPi).

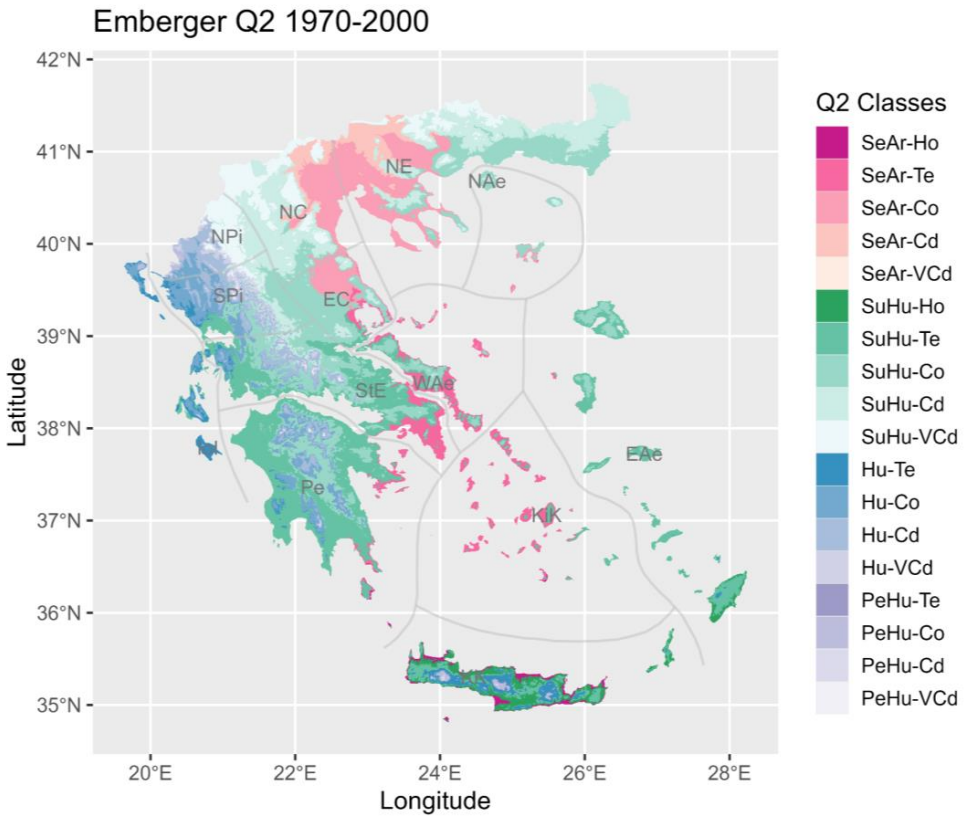

Figure 4. Spatial distribution of the Emberger Q2 classes for the reference period (1970–2000) over the phytogeographical regions of Greece.

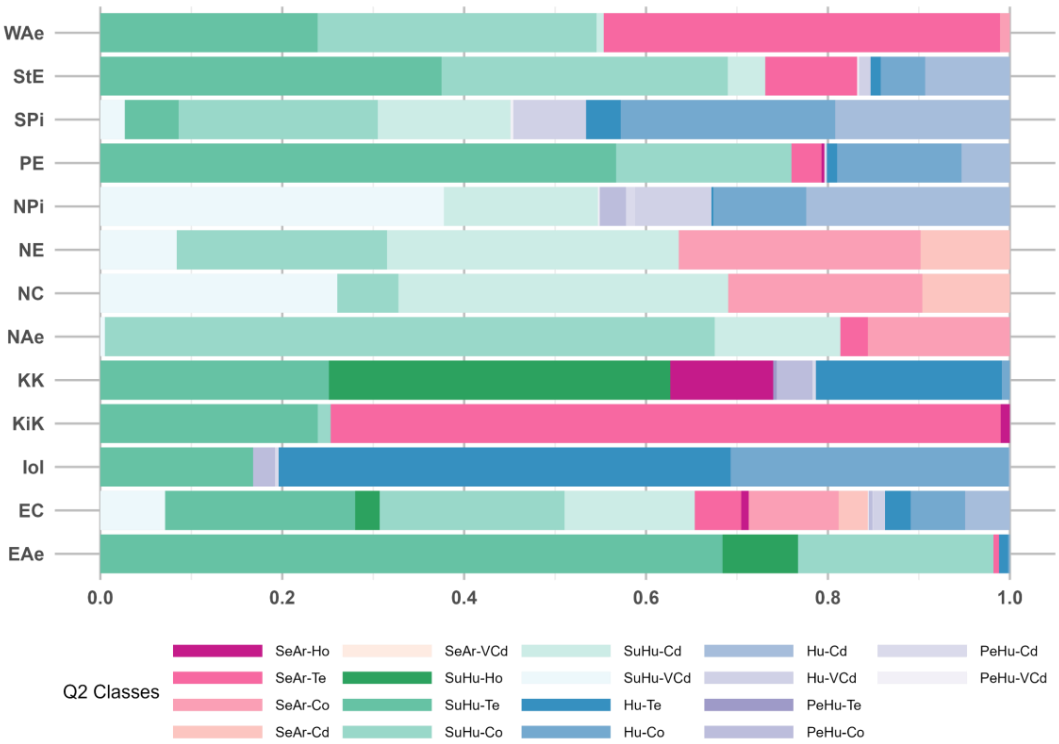

Figure 5. Q2 classes' relative surface (1 = 100%) per phytogeographical region for the reference period (1970–2000).

3.2. Emissions Scenario RCP4.5 for the 2021–2040 Time Period

In comparison with the Ref (1970–2000) (Figure 4), classifications of the Q1 for the 2021–2040 timeframe (henceforth P1) under the RCP4.5 scenario reveal distributions among the same bioclimate types (PeHu, Hu, SuHu, and SeAr) (Figure S3). However, xerothermic trends are already evident in this relatively short-term period, given the % coverage favoring the SeAr and SuHu classes in contradiction to the distribution decrease in the Hu and PeHu classes. The drier and warmer bioclimatic conditions of the SeAr class are expected to spatially expand (Figure S4 and Table S2), mostly over the phytogeographical regions of the North East (NE) (from 68% in the Ref to 84%) and the North Aegean Islands (NAe) (from 58% to 68%). This is also the case for the SuHu class, which appears more distributed over the Northern Pindos (NPi) and Southern Pindos (SPi) (64% to 75% and 70% to 82%, respectively).

The drying and warming trend over the Greek territory is already evident from the first period of the less influential RCP4.5 scenario. With respect to the Ref, Figure 5 demonstrates that, in the short run, additional xerothermal conditions may influence mainly southern Greece (e.g., the SeAr-VHo in KK). Comparisons of the outcomes on the Q2 classes' relative % coverage per phytogeographical region in P1 (Figures 6 and 7 and Table S7) with the respective in the Ref (Figure 4 and Table S6) reveal significant increases in the SeAr-Ho subtype for the KK region (11% in Ref to 27% in P1) and majorly for the KiK region (1% in Ref to 64% in P1). Also, the EAe, NAe, WAe, and NE regions are foreseen to experience substantial dry–thermal changes owing to the spatial increases of the SeAr-Te (e.g., 0.6% to nearly 10% for the EAe, 3% to 59% for the NAe, 44% to 68% for the WAe, 0% to 35% for the NE). A notable increase is also exhibited for the SuHu-Ho category over the EAe region (from 8% in Ref to 38% in P1).

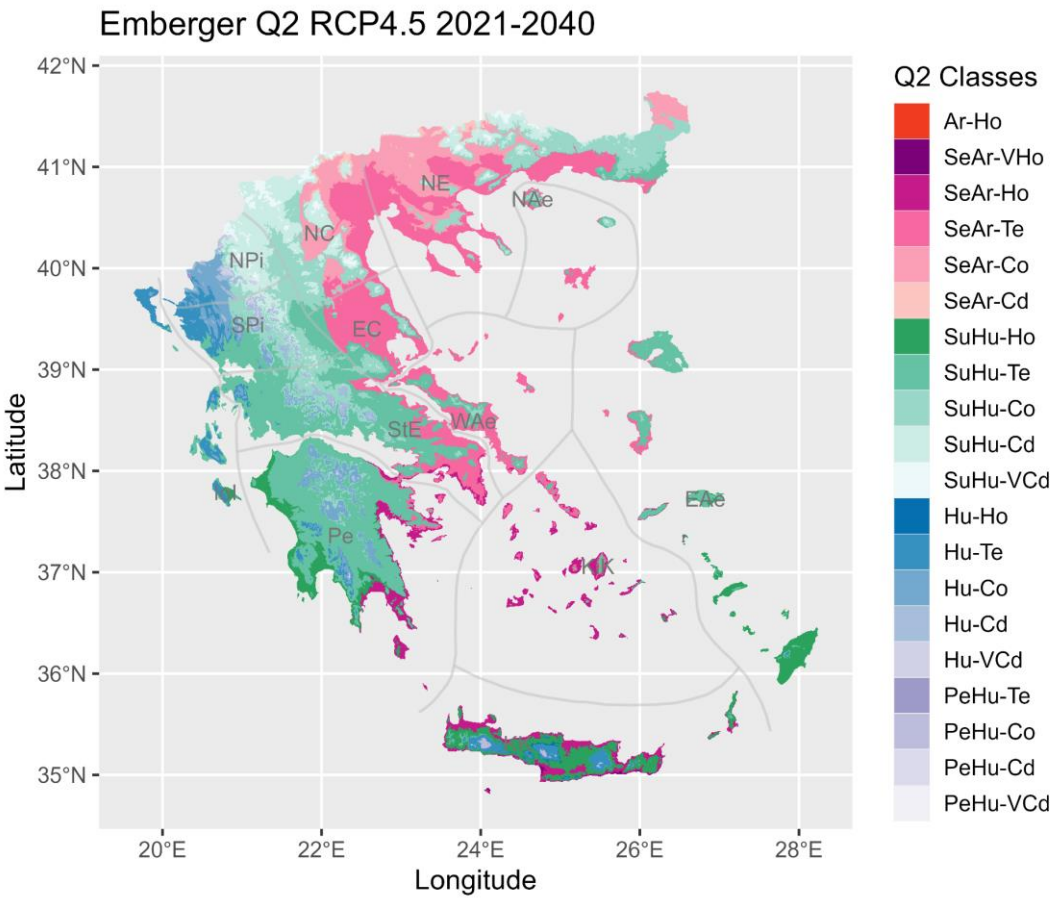

Figure 6. Spatial distribution of the Emberger Q2 classes for the RCP4.5 scenario and 2021–2040 period over the phytogeographical regions of Greece.

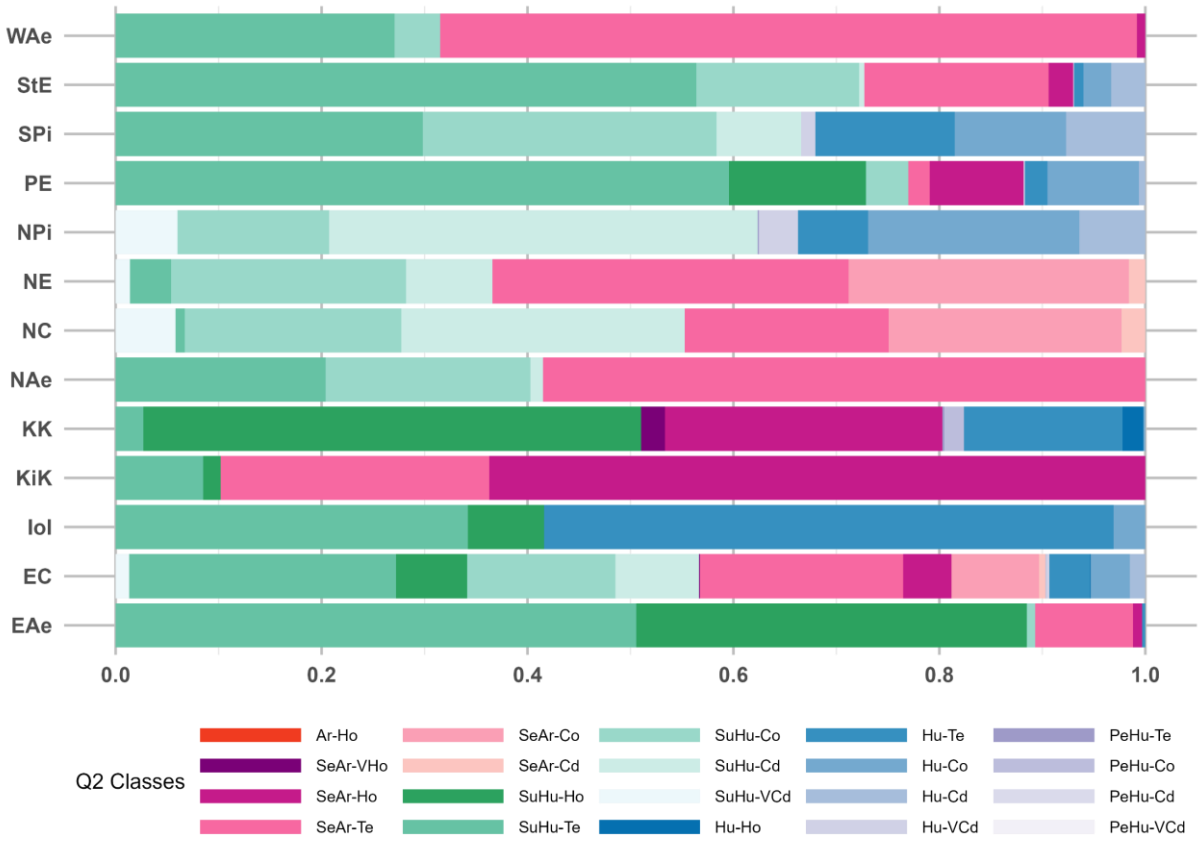

Figure 7. Q2 classes' relative surface (1 = 100%) per phytogeographical region for the RCP4.5 scenario and 2021–2040 period.

3.3. Emissions Scenario RCP4.5 for the 2041–2060 Time Period

As illustrated in Figure S5, outcomes on the 2nd investigated period (henceforth P2) of the RCP4.5 demonstrate the possible existence in the long run of the four Q1 main classes (PeHu, Hu, SuHu and SeAr), which also occur for the Ref and P1 (Figures S1 and S3, respectively). With reference to the latter periods, an important % coverage decrease in the Hu type is documented for, e.g., the IoI phytogeographical region (65% in Ref to 53% in P1 and 27% in P2) in favor of the less humid SuHu class (35% in Ref to 47% in P1 and 73% in P2). In comparison with the Ref, more xerothermic conditions are exhibited due to significant increases resulting for the SeAr type over the NE (from 68% in Ref to 90% in P2), the NC (49% to 69%), and the NAe (58% to 79%) phytogeographical regions.

Overall, a more intense dry–thermal trend is documented for the P2 of the RCP4.5 compared with the P1 and the Ref. Although distributed among the same Q2 classes (Figures 8 and 9 vs. Figures 4 and 6), the bioclimate is now characterized also by the warmer SuHu-VHo while the PeHu-VCd occurring in the previous RCP4.5 timeframes is now out of the picture. In addition, with reference to the preceding time periods (Ref and P1), 19% coverage of the SeAr-VHo class occurs for the first time in the KK region. A more than tenfold % increase in the SeAr-Ho is also documented in the WAe region (0.8% in P1 to 12% in P2). Furthermore, an apparent more dry–thermal evolution is illustrated due to the presence of the SeAr-Te bioclimate, which now appears to influence greater areas of the NAe region (3% in Ref to 59% in P1 and 75% in P2) and the NE region (35% in P1 to 49% in P2).

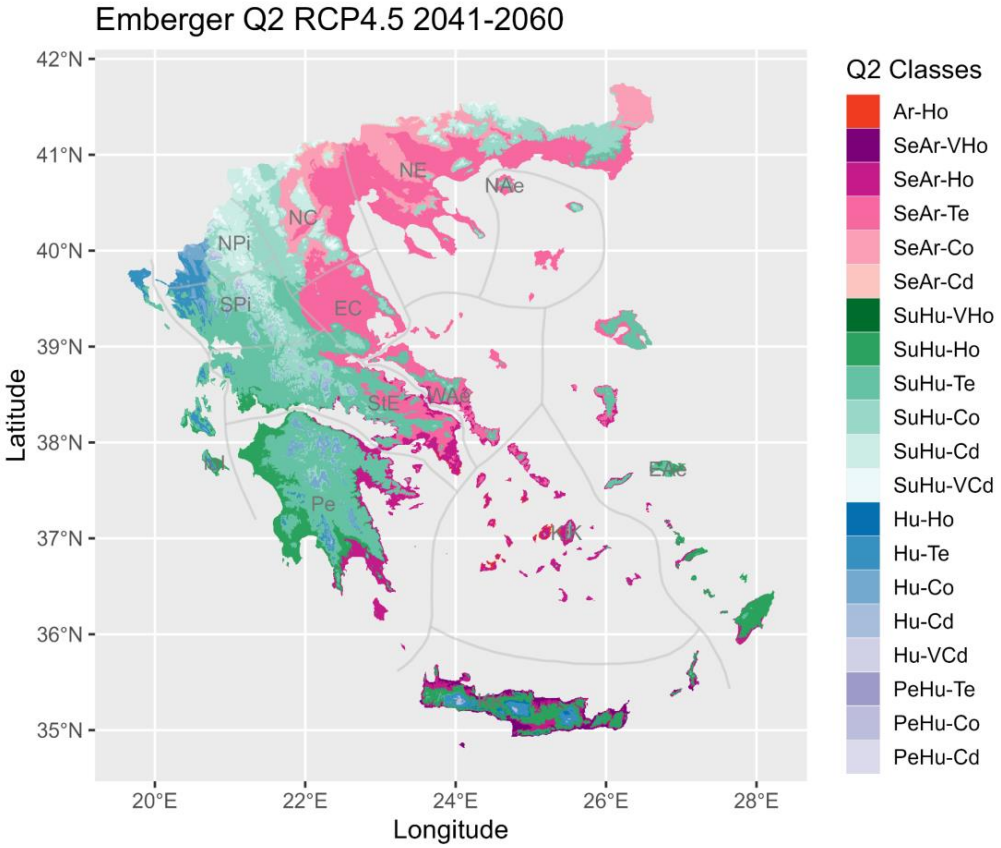

Figure 8. Spatial distribution of the Emberger Q2 classes for the RCP4.5 scenario and 2041–2060 period over the phytogeographical regions of Greece.

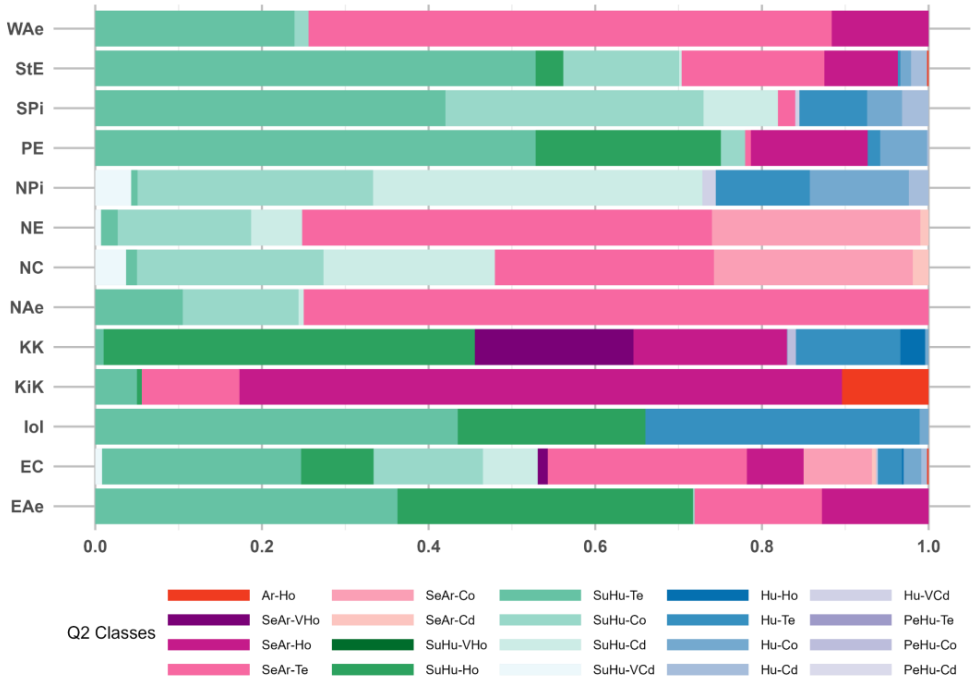

Figure 9. Q2 classes' relative surface (1 = 100%) per phytogeographical region for the RCP4.5 scenario and 2041–2060 period.

3.4. Emissions Scenario RCP8.5 for the 2021–2040 Time Period

Under the RCP8.5, the Emberger Q1 classifications for the P1 (2021–2040) exhibit almost identical spatial patterns (Figure S7) with the P2 (2041–2060) of the RCP4.5 scenario (Figure S5). This similarity pinpoints the crucial role of the more extreme RCP8.5 by considering the notable advancement of its bioclimatic negative impacts. As already demonstrated for the P2 of the RCP4.5, the same bioclimate types (PeHu, Hu, SuHu, and SeAr) are now evident, while significant increases also result for the SeAr type over the NE (68% in Ref to 88%), the NC (49% to 64%), and the NAe (58% to 76%) phytogeographical regions. Similarly to the P2 of the RCP4.5, a significant % coverage increase in the less humid SuHu type (35% in Ref to 67%) at the expense of the Hu type (65% in Ref to 33%) results for the region of the Ionian Islands (IoI).

For this examined case, similarities with the P2 of the RCP4.5 on the characterization of the bioclimate resulting in the same 20 Q2 classes are also demonstrated (Figure 10 vs. Figure 8). Related results on the % Q2 classes coverage per phytogeographical regions are also evident under the RCP8.5 (Figure 11 vs. Figure 9 and Table S9 vs. Table S8). A few exceptions, however, involve more limited occurrences, mainly of the SeAr-VHo (8% in the P1 of the RCP8.5 vs. 19% in the P2 of the RCP4.5 over the KK), the SeAr-Ho (e.g., 1.3% vs. 13% for the EAe, 1.2% vs. 12% for the WAe), and the SeAr-Te classes (65% vs. 75% for the NAe and 33% vs. 49% for the NE). Concomitantly, more extensive % coverage occurs as displayed for the SeAr-Te conditions over the KiK phytogeographical region (24% vs. 12%).

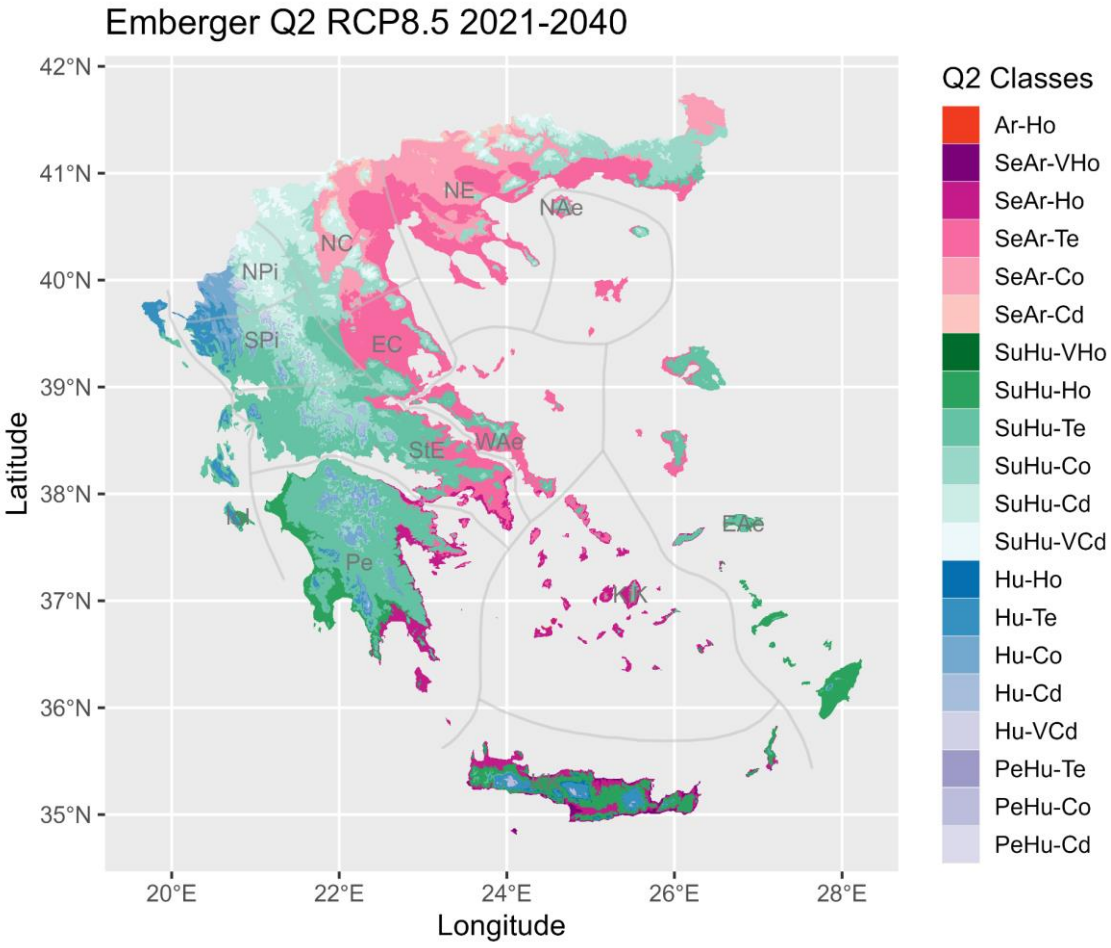

Figure 10. Spatial distribution of the Emberger Q2 classes for the RCP8.5 scenario and the 2021–2040 period over the phytogeographical regions of Greece.

Figure 11. Q2 classes relative surface (1 = 100%) per phytogeographical region for the RCP8.5 scenario and 2021–2040 period.

3.5. Emissions Scenario RCP8.5 for the 2041–2060 Time Period

The more intensified drying and warming of the Greek bioclimate is clearly demonstrated over the P2 (2041–2060) of the RCP8.5 scenario. In this case, three Q1 categories are distinguished (Hu, SuHu, and SeAr) since the most humid PeHu bioclimatic type is now absent for the first time (Figure S9). On the contrary, an increase in the % coverage of the most arid SeAr class is exhibited over all the phytogeographical regions with respect to all previous cases (e.g., Figure S10 vs. Figure S8 and Table S5 vs. Table S4). When compared with the reference period, most impacted phytogeographical regions by the SeAr conditions include the NC (from approximately 49% in the Ref to 74% in the P2 of the RCP8.5), NE (68% to 93%), NAe (58% to 81%), WAe (56% to 76%), KiK (67% to 81%), EC (29% to 42%), and the StE (11% to 20%).

With reference to the P1 of the RCP8.5 (Figure 12 vs. Figure 10), the appearance for the first time of the Ar-VHo Q2 subtype (almost 1% coverage over the KK region) (Figure 13 and Table S10) and the concomitant absence of the PeHu-Te may justify more intense xerothermic trends. The present case results as the most influential by accounting the substantial spatial pattern evolution of the more dry–thermal Q2 classes and mainly of the Ar-Ho (from 0.7% in the P1 of the RCP8.5 to 29% over the KiK), the SeAr-VHo (8% to 30% over the KK), the SeAr-Ho (1.2% to 26% in the WAe), and the SeAr-Te (e.g., 33% to 56% in the NE; 19% to 31% in the NC).

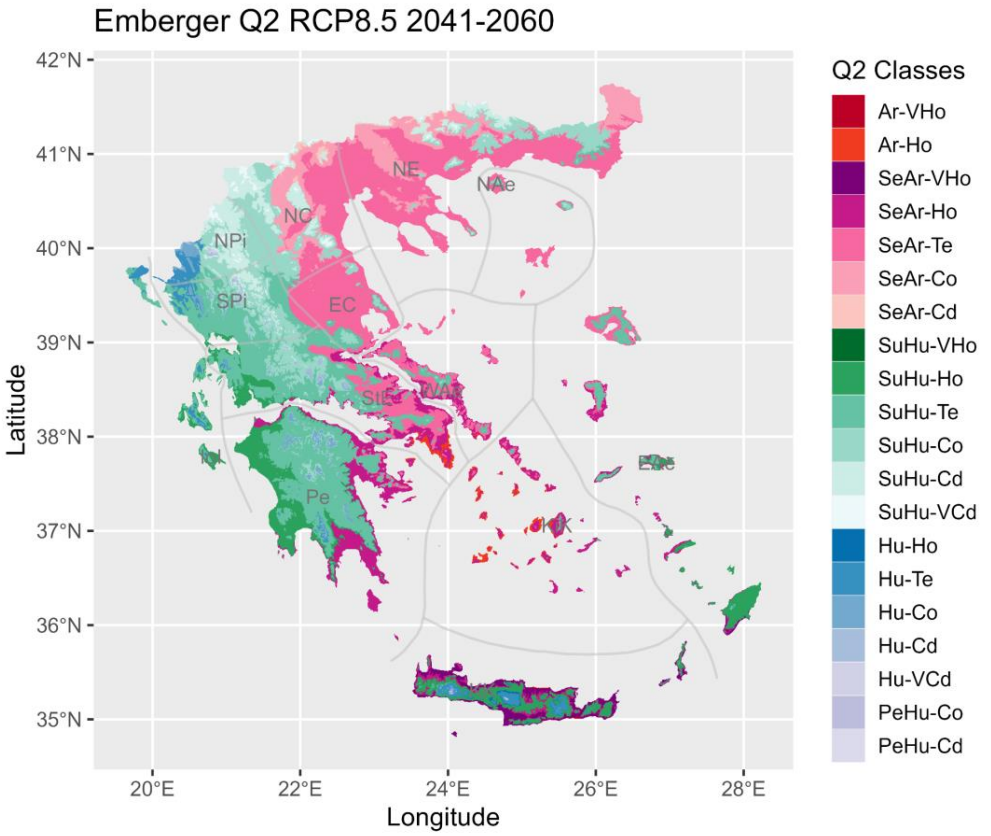

Figure 12. Spatial distribution of the Emberger Q classes for the RCP8.5 scenario and the 2041–2060 period over the phytogeographical regions of Greece.

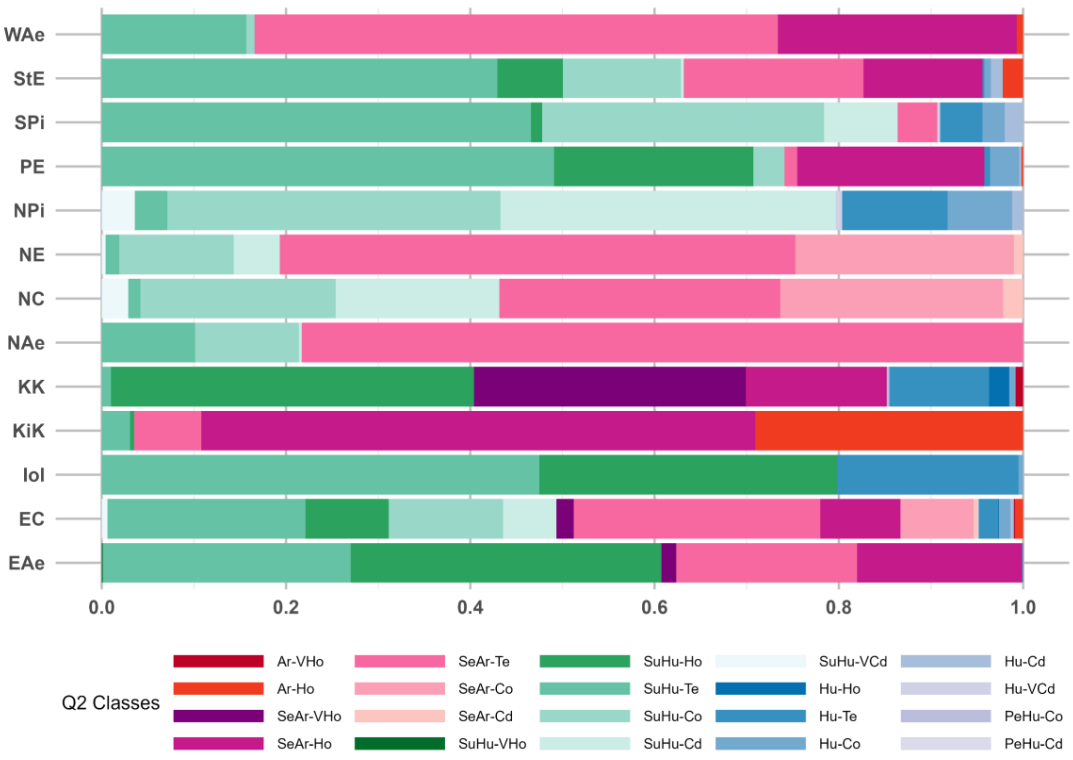

Figure 13. Q2 classes' relative surface (1 = 100%) per phytogeographical region for the RCP8.5 scenario and 2041–2060 period.

3.6. Management Implications

The study findings render significant bioclimatic changes throughout Greece. Especially the expansion of the Arid-Hot, Semi-Arid–Very Hot, Semi-Arid–Hot, and Semi-Arid–Temperate Q2 classes, respectively, over the phytogeographical regions of Kiklades (up to 29% occupation), Kriti and Karpathos (up to 30%), West Aegean Islands (up to 26%), North East (up to 56%), and North Central (up to 31%), by 2060 (RCP8.5), highlights a severe threat to flora species and vegetation, especially in the island regions and in the mountain tops (the "escalator to extinction" phenomenon). Findings from the RCP8.5 long-term scenario support that the east part of Greece will have a more dry–thermal bioclimate, thus threatening spatial shifts or even the extinction of species and vegetation communities (see, e.g., [38,118,119]). Our findings on the impact of CC on Greece's phytogeographical regions extend to the alteration of phenological events. Phenology, the study of periodic plant and animal life cycle events, is highly sensitive to climate changes. For instance, earlier flowering of plants can disrupt the synchrony between plants and their pollinators, affecting pollination success and, consequently, plant reproduction [120]. Grillakis et al. [120] emphasize that the earlier flowering of olive trees in Crete due to CC can have significant implications for olive production and the broader ecosystem.

One of the critical areas affected by bioclimate change in Greece is documented at the Chelmos-Vouraikos National Park, a regional biodiversity hotspot in the northern part of the phytogeographical region of Peloponnisos (Pe); the study by Kougioumoutzis et al. [121] highlights the significant impacts of climate and land-cover change on rare and endemic species distributions within this park. The study emphasizes that changes in temperature and precipitation patterns, coupled with human-induced land-cover changes, pose substantial risks to the survival of these species. Using extinction risk assessment models to predict the future viability of these taxa under various climate scenarios, the researchers found that many species may face increased extinction risks unless proactive conservation measures are implemented.

Additionally, we should note that the conservation of Mediterranean phytogeographical diversity in areas like the island of Crete, included in the phytogeographical region of Kriti and Karpathos (KK), is closely linked to traditional land use practices. Siebert [122] argues that maintaining traditional cultivation and livestock grazing practices is crucial for preserving the mosaic of habitats supporting high biodiversity levels. These practices help maintain the structural complexity and heterogeneity of the landscape, which are vital for supporting diverse plant communities. The abandonment of traditional agricultural practices, driven by socio-economic changes, poses a threat to this biodiversity, as it leads to habitat homogenization and the loss of species adapted to these traditional land-use systems [122].

In peri-urban areas, such as the forests surrounding the city of Thessaloniki, belonging to the phytogeographical region of North East (NE) Greece, the change of the bioclimate and the anthropogenic activities have led to significant degradation of phytogeographical quality. Petaloudi et al. [123] report that forest fragmentation, pollution, and the presence of garbage have varying degrees of negative impacts on forest ecosystem types. The study highlights that different forest ecosystems within the peri-urban area exhibit varying levels of degradation and biodiversity status, with some areas showing considerable declines in species diversity and forest health. This degradation is exacerbated by the increasing urban heat island effect and changing precipitation patterns, which further stress these ecosystems.

Agroecosystems in regions like East Attiki Prefecture, belonging to the phytogeographical region of Sterea Ellas (StE), play a crucial role in preserving plant diversity. Spanou et al. [124] explore the phytogeographical and vegetation diversity within these agroecosystems, finding that they significantly contribute to the area's overall plant diversity. These systems can serve as vital reservoirs of biodiversity, supporting a wide range of plant species that are adapted to specific agricultural practices. The study underscores the importance of integrating biodiversity conservation into agricultural land management

to ensure the sustainability of these ecosystems, which can be significantly altered by the predicted shift in the bioclimate in the region.

The phenotypic diversity of certain species, such as *Sideritis scardica* in Northern Greece (mainly in phytogeographical regions of NC and NE), is closely linked to the phytogeographical composition of their habitats. Papaporfyriou et al. [125] found that the presence of specific plant groups, like forbs, can favor the abundance and diversity of *Sideritis scardica* populations, whereas high densities of graminoid and shrub species can suppress their presence. This interaction between species highlights the complex dynamics within plant communities and the importance of habitat composition in maintaining species diversity [125], a condition that will be severely affected by predicted bioclimate shifts.

4. Conclusions

Bioclimate change, driven primarily by human activities, has significant and far-reaching impacts on the floristic diversity of various regions. These impacts are particularly pronounced in Greece, a country characterized by rich biodiversity and distinct ecological zones. The following conclusions may summarize the innovative findings of the present study.

Greece is projected to face drier and warmer conditions under both scenarios (RCP4.5 and RCP8.5).

It also appears that for both emission scenarios, the bioclimate of Greece temporarily becomes more xerothermic given the resulting gradual drier and warmer transitions between the studied timeframes (reference period: 1970–2000, 1st time period: 2021–2040 and 2nd time period: 2041–2060). Classifications of the Q1 type under the RCP4.5 scenario reveal distributions among four bioclimate types (PeHu, Hu, SuHu, and SeAr) independently of the examined time frame. Classifications of the Q2 subtypes (20 in total), however, demonstrate the appearance of more xerothermic categories (Ar-Ho, SeAr-VHo, HuHo, and SuHu-VHo), the spatial distributions of which are primarily evident during the investigated long-term time period (2041–2060).

Under the RCP4.5, the phytogeographical regions, which appear mostly drier and warmer in the more distant future (2041–2060), are almost entirely located in the right half of the country. By 2060, under the RCP4.5 scenario, the SeAr-Te bioclimate type is expected to dominate the NAe and WAe phytogeographical regions, while the more xerothermic SeAr-Hot will influence most of the KiK region and parts of the WAe, StE, PE, KK, EC, and EAe regions. It is also underlined that, even under the less influential RCP4.5, even more adverse conditions of the SeAr-VHot class may be present in the KK and EC regions. The same Emberger Q1 classifications in the 2021–2040 period of the extreme RCP8.5 (4 bioclimate types: PeHu, Hu, SuHu, and SeAr) are demonstrated and exhibit similar spatial distributions with the respective ones for the 2041–2060 period of the RCP4.5 scenario. The xerothermic trends' similarity between these cases highlights the crucial role of the more extreme RCP8.5 owing to the pronounced advancement of its impacts on the investigated area's bioclimate. Classifications of the Q2 fall within the aforenamed Ar-Ho, SeAr-VHo, HuHo, and SuHu-VHo, forming once more the same types (also 20 in total) and relatively similar spatial distributions per phytogeographical region with some exceptions concerning the SeAr categories.

The most impactful is the 2nd period (2041–2060) of the RCP8.5 scenario, which is projected to induce substantial drying and warming over the investigated area. Three Hu, SuHu, and SeAr subtypes are determined, while an increase in the latter's % coverage (most xerothermic SeAr) is exhibited over all geographical zones. Concerning the 1970–2000 period, the areas most impacted by the SeAr conditions are the NC, NE, NAe, WAe, KiK, EC, and the StE phytogeographical regions. As for the % spatial coverage of the Q2 types, a small expansion of the Ar-VHo and the absence of the PeHu-Te both justify more intense dry–thermal trends. The latter trends are clear given the significant spatial evolution mainly of the Ar-Ho, SeAr-VHo, SeAr-Ho, and SeAr-Te classes, respectively, over the KiK, KK, WAe, NE–NC regions, which is projected to occur by 2060 under the RCP8.5.

It is evident that the long-term time period (2041–2060) of the extreme RCP8.5 scenario exhibits the strongest dry–thermal trends over the eastern half of the Greek territory. The alteration of the bioclimate can be characterized as one of the most tenacious and pressing threats to the ecosystems over the Greek territory. Its impacts are expected to pose substantial threats to the phytogeographical regions of Greece, impacting agriculture, forest health, national parks and protected areas, urban environments, and phenological events related to the now-established flora and vegetation. Our study highlights the need for comprehensive strategies to mitigate and adapt to CC, urging decision-makers efforts to focus on sustainable agricultural practices, forest management, urban planning, and conservation of biodiversity to safeguard Greece's rich floristic heritage and natural capital in the face of a changing climate.

Supplementary Materials: The following supporting information can be downloaded at: https://zenodo.org/doi/10.5281/zenodo.12597897 (accessed on 29 June 2024), Figure S1: Spatial distribution of Emberger Q1 classes for the reference period (1970–2000) over the phytogeographical zones of Greece.; Figure S2. Q1 classes relative surface (1.0 = 100%) per phytogeographical zone for the reference period (1970–2000); Table S1. The percentage (%) of Q1 classes coverage per phytogeographical zone for the 1970–2000 period; Figure S3. Spatial distribution of Emberger Q1 classes for RCP4.5 scenario and 2021–2040 period over the phytogeographical zones of Greece; Figure S4. Q1 classes relative surface (1.0 = 100%) per phytogeographical zone for RCP4.5 scenario and 2021–2040 period; Table S2. The percentage (%) of Q1 classes coverage per phytogeographical zone for RCP4.5 scenario and 2021–2040 period; Figure S5. Spatial distribution of Emberger Q classes for RCP4.5 scenario and 2041–2060 period over the phytogeographical zones of Greece; Figure S6. Q1 classes relative surface (1.0 = 100%) per phytogeographical zone for RCP4.5 scenario and 2041–2060 period; Table S3. The percentage (%) of Q1 classes coverage per phytogeographical zone for RCP4.5 scenario and 2041–2060 period; Figure S7. Spatial distribution of Emberger Q1 classes for RCP8.5 scenario and 2021–2040 period over the phytogeographical zones of Greece; Figure S8. Q1 classes relative surface (1.0 = 100%) per phytogeographical zone for RCP8.5 scenario and 2021–2040 period; Table S4. The percentage (%) of Q1 classes coverage per phytogeographical zone for RCP8.5 scenario and 2021–2040 period; Figure S9. Spatial distribution of Emberger Q1 classes for RCP8.5 scenario and 2041–2060 period over the phytogeographical zones of Greece; Figure S10. Q1 classes relative surface (1.0 = 100%) per phytogeographical zone for RCP8.5 scenario and 2041–2060 period; Table S5. The percentage (%) of Q1 classes coverage per phytogeographical zone for RCP8.5 scenario and 2041–2060 period; Table S6. The percentage (%) of Q2 classes coverage per phytogeographical zone for the 1970–2000 period; Table S7. The percentage (%) of Q2 classes coverage per phytogeographical zone for the RCP4.5 2021–2040 period; Table S8. The percentage (%) of Q2 classes coverage per phytogeographical zone for the RCP4.5 2041–2060 period; Table S9. The percentage (%) of Q2 classes coverage per phytogeographical zone for the RCP8.5 2021–2040 period; Table S10. The percentage (%) of Q2 classes coverage per phytogeographical zone for the RCP8.5 2041–2060 period.

Author Contributions: Conceptualization, I.C. and I.P.K.; Methodology, I.C.; Investigation, F.D. and I.C.; Resources, F.D.; Original Preparation and Writing, F.D.; Writing on Data and Methods, I.C.; Method Application and computation of Results, I.C.; Table and Figures, I.C.; Writing on Results, F.D.; Writing Discussion for natural areas implications and policies I.P.K. and P.D. Writing-Review and Editing, F.D., I.P.K. and P.D. All authors have read and agreed to the published version of the manuscript.

Funding: This research received no external funding.

Data Availability Statement: Ultra-high resolution maps that are presented in this study are available upon request.

Conflicts of Interest: The authors declare no conflicts of interest.

References

1. Pörtner, H.-O.; Roberts, D.C.; Tignor, M.; Poloczanska, E.S.; Mintenbeck, K.; Alegria, A.; Craig, M.; Langsdorf, S.; Löschke, S.; Möller, V.; et al. *Climate Change 2022: Impacts, Adaptation and Vulnerability. Contribution of Working Group II to the Sixth Assessment Report of the Intergovernmental Panel on Climate Change*; Cambridge University Press: Cambridge, UK; New York, NY, USA, 2022; ISBN 978-1-00-932584-4.
2. Charalampopoulos, I.; Droulia, F. The Agro-Meteorological Caused Famines as an Evolutionary Factor in the Formation of Civilisation and History: Representative Cases in Europe. *Climate* **2021**, *9*, 5. [CrossRef]
3. Matzarakis, A. Comments about Urban Bioclimate Aspects for Consideration in Urban Climate and Planning Issues in the Era of Climate Change. *Atmosphere* **2021**, *12*, 546. [CrossRef]
4. Giannetto, D.; Innal, D. Status of Endemic Freshwater Fish Fauna Inhabiting Major Lakes of Turkey under the Threats of Climate Change and Anthropogenic Disturbances: A Review. *Water* **2021**, *13*, 1534. [CrossRef]
5. Skendžić, S.; Zovko, M.; Živković, I.P.; Lešić, V.; Lemić, D. The Impact of Climate Change on Agricultural Insect Pests. *Insects* **2021**, *12*, 440. [CrossRef] [PubMed]
6. Orgeret, F.; Thiebault, A.; Kovacs, K.M.; Lydersen, C.; Hindell, M.A.; Thompson, S.A.; Sydeman, W.J.; Pistorius, P.A. Climate Change Impacts on Seabirds and Marine Mammals: The Importance of Study Duration, Thermal Tolerance and Generation Time. *Ecol. Lett.* **2022**, *25*, 218–239. [CrossRef]
7. Droulia, F.; Charalampopoulos, I. A Review on the Observed Climate Change in Europe and Its Impacts on Viticulture. *Atmosphere* **2022**, *13*, 837. [CrossRef]
8. Charalampopoulos, I.; Droulia, F.; Tsiros, I.X. Projecting Bioclimatic Change over the South-Eastern European Agricultural and Natural Areas via Ultrahigh-Resolution Analysis of the de Martonne Index. *Atmosphere* **2023**, *14*, 858. [CrossRef]
9. Charalampopoulos, I.; Droulia, F.; Kokkoris, I.P.; Dimopoulos, P. Future Bioclimatic Change of Agricultural and Natural Areas in Central Europe: An Ultra-High Resolution Analysis of the De Martonne Index. *Water* **2023**, *15*, 2563. [CrossRef]
10. Vlami, V.; Kokkoris, I.P.; Charalampopoulos, I.; Doxiadis, T.; Giannakopoulos, C.; Lazoglou, M. A Transect Method for Promoting Landscape Conservation in the Climate Change Context: A Case-Study in Greece. *Sustainability* **2023**, *15*, 13266. [CrossRef]
11. Weiskopf, S.R.; Rubenstein, M.A.; Crozier, L.G.; Gaichas, S.; Griffis, R.; Halofsky, J.E.; Hyde, K.J.W.; Morelli, T.L.; Morisette, J.T.; Muñoz, R.C.; et al. Climate Change Effects on Biodiversity, Ecosystems, Ecosystem Services, and Natural Resource Management in the United States. *Sci. Total Environ.* **2020**, *733*, 137782. [CrossRef]
12. Nhemachena, C.; Nhamo, L.; Matchaya, G.; Nhemachena, C.R.; Muchara, B.; Karuaihe, S.T.; Mpandeli, S. Climate Change Impacts on Water and Agriculture Sectors in Southern Africa: Threats and Opportunities for Sustainable Development. *Water* **2020**, *12*, 2673. [CrossRef]
13. Charalampopoulos, I.; Droulia, F. A Pathway towards Climate Services for the Agricultural Sector. *Climate* **2024**, *12*, 18. [CrossRef]
14. Droulia, F.; Charalampopoulos, I. Future Climate Change Impacts on European Viticulture: A Review on Recent Scientific Advances. *Atmosphere* **2021**, *12*, 495. [CrossRef]
15. Koufos, G.C.; Mavromatis, T.; Koundouras, S.; Jones, G.V. Response of Viticulture-Related Climatic Indices and Zoning to Historical and Future Climate Conditions in Greece. *Int. J. Climatol.* **2018**, *38*, 2097–2111. [CrossRef]
16. Feidas, H. Trend Analysis of Air Temperature Time Series in Greece and Their Relationship with Circulation Using Surface and Satellite Data: Recent Trends and an Update to 2013. *Theor. Appl. Climatol.* **2017**, *129*, 1383–1406. [CrossRef]
17. Charalampopoulos, I.; Droulia, F.; Evans, J. The Bioclimatic Change of the Agricultural and Natural Areas of the Adriatic Coastal Countries. *Sustainability* **2023**, *15*, 4867. [CrossRef]
18. Georgoulias, A.K.; Akritidis, D.; Kalisoras, A.; Kapsomenakis, J.; Melas, D.; Zerefos, C.S.; Zanis, P. Climate Change Projections for Greece in the 21st Century from High-Resolution EURO-CORDEX RCM Simulations. *Atmos. Res.* **2022**, *271*, 106049. [CrossRef]
19. Zanis, P.; Katragkou, E.; Ntogras, C.; Marougianni, G.; Tsikerdekis, A.; Feidas, H.; Anadranistakis, E.; Melas, D. Transient High-Resolution Regional Climate Simulation for Greece over the Period 1960-2100: Evaluation and Future Projections. *Clim. Res.* **2015**, *64*, 123–140. [CrossRef]
20. Katopodis, T.; Markantonis, I.; Vlachogiannis, D.; Politi, N.; Sfetsos, A. Assessing Climate Change Impacts on Wind Characteristics in Greece through High Resolution Regional Climate Modelling. *Renew. Energ.* **2021**, *179*, 427–444. [CrossRef]
21. Giannakopoulos, C.; Kostopoulou, E.; Varotsos, K.V.; Tziotziou, K.; Plitharas, A. An Integrated Assessment of Climate Change Impacts for Greece in the near Future. *Reg. Environ. Chang.* **2011**, *11*, 829–843. [CrossRef]
22. Kourgialas, N.N.; Karatzas, G.P. A Flood Risk Decision Making Approach for Mediterranean Tree Crops Using GIS.; Climate Change Effects and Flood-Tolerant Species. *Environ. Sci. Policy* **2016**, *63*, 132–142. [CrossRef]
23. Anagnostopoulou, C. Drought Episodes over Greece as Simulated by Dynamical and Statistical Downscaling Approaches. *Theor. Appl. Climatol.* **2017**, *129*, 587–605. [CrossRef]
24. Galanaki, E.; Giannaros, C.; Kotroni, V.; Lagouvardos, K.; Papavasileiou, G. Spatio-Temporal Analysis of Heatwaves Characteristics in Greece from 1950 to 2020. *Climate* **2023**, *11*, 5. [CrossRef]
25. Nastos, P.T.; Kapsomenakis, J. Regional Climate Model Simulations of Extreme Air Temperature in Greece. Abnormal or Common Records in the Future Climate? *Atmos. Res.* **2015**, *152*, 43–60. [CrossRef]
26. Founda, D.; Varotsos, K.V.; Pierros, F.; Giannakopoulos, C. Observed and Projected Shifts in Hot Extremes' Season in the Eastern Mediterranean. *Glob. Planet. Chang.* **2019**, *175*, 190–200. [CrossRef]

27. Koulelis, P.P.; Proutsos, N.; Solomou, A.D.; Avramidou, E.V.; Malliarou, E.; Athanasiou, M.; Xanthopoulos, G.; Petrakis, P.V. Effects of Climate Change on Greek Forests: A Review. *Atmosphere* **2023**, *14*, 1155. [CrossRef]
28. CCISC Climate Change Impacts Study Committee. *The Environmental, Economic and Social Impacts of Climate Change in Greece*; Bank of Greece Eurosystem: Athens, Greece, 2011; ISBN 978-960-7032-58-4.
29. Angra, D.; Sapountzaki, K. Climate Change Affecting Forest Fire and Flood Risk—Facts, Predictions, and Perceptions in Central and South Greece. *Sustainability* **2022**, *14*, 13395. [CrossRef]
30. Politi, N.; Vlachogiannis, D.; Sfetsos, A.; Gounaris, N.; Varela, V. Investigation of Fire Weather Danger under a Changing Climate at High Resolution in Greece. *Sustainability* **2023**, *15*, 2498. [CrossRef]
31. Mitsopoulos, I.; Mallinis, G.; Karali, A.; Giannakopoulos, C.; Arianoutsou, M. Mapping Fire Behaviour under Changing Climate in a Mediterranean Landscape in Greece. *Reg. Environ. Chang.* **2016**, *16*, 1929–1940. [CrossRef]
32. Rovithakis, A.; Grillakis, M.G.; Seiradakis, K.D.; Giannakopoulos, C.; Karali, A.; Field, R.; Lazaridis, M.; Voulgarakis, A. Future Climate Change Impact on Wildfire Danger over the Mediterranean: The Case of Greece. *Environ. Res. Lett.* **2022**, *17*, 045022. [CrossRef]
33. Stefanidis, S.; Dafis, S.; Stathis, D. Evaluation of Regional Climate Models (RCMs) Performance in Simulating Seasonal Precipitation over Mountainous Central Pindus (Greece). *Water* **2020**, *12*, 2750. [CrossRef]
34. Papadopoulos, A. Tree-Ring Patterns and Climate Response of Mediterranean Fir Populations in Central Greece. *Dendrochronologia* **2016**, *40*, 17–25. [CrossRef]
35. Kastridis, A.; Kamperidou, V.; Stathis, D. Dendroclimatological Analysis of Fir (*A. borisii-regis*) in Greece in the Frame of Climate Change Investigation. *Forests* **2022**, *13*, 879. [CrossRef]
36. Chrysopolitou, V.; Apostolakis, A.; Avtzis, D.; Avtzis, N.; Diamandis, S.; Kemitzoglou, D.; Papadimos, D.; Perlerou, C.; Tsiaoussi, V.; Dafis, S. Studies on Forest Health and Vegetation Changes in Greece under the Effects of Climate Changes. *Biodivers. Conserv.* **2013**, *22*, 1133–1150. [CrossRef]
37. Kokkoris, I.P.; Kougioumoutzis, K.; Charalampopoulos, I.; Apostolidis, E.; Apostolidis, I.; Strid, A.; Dimopoulos, P. Conservation Responsibility for Priority Habitats under Future Climate Conditions: A Case Study on *Juniperus drupacea* Forests in Greece. *Land* **2023**, *12*, 1976. [CrossRef]
38. Kougioumoutzis, K.; Kokkoris, I.P.; Panitsa, M.; Trigas, P.; Strid, A.; Dimopoulos, P. Plant Diversity Patterns and Conservation Implications under Climate-Change Scenarios in the Mediterranean: The Case of Crete (Aegean, Greece). *Diversity* **2020**, *12*, 270. [CrossRef]
39. Stathi, E.; Kougioumoutzis, K.; Abraham, E.M.; Trigas, P.; Ganopoulos, I.; Avramidou, E.V.; Tani, E. Population Genetic Variability and Distribution of the Endangered Greek Endemic *Cicer Graecum* under Climate Change Scenarios. *AoB PLANTS* **2020**, *12*, plaa007. [CrossRef]
40. Fyllas, N.M.; Koufaki, T.; Sazeides, C.I.; Spyroglou, G.; Theodorou, K. Potential Impacts of Climate Change on the Habitat Suitability of the Dominant Tree Species in Greece. *Plants* **2022**, *11*, 1616. [CrossRef]
41. Zindros, A.; Radoglou, K.; Milios, E.; Kitikidou, K. Tree Line Shift in the Olympus Mountain (Greece) and Climate Change. *Forests* **2020**, *11*, 985. [CrossRef]
42. Christopoulou, A.; Christopoulou, A.; Fyllas, N.M.; Dimitrakopoulos, P.G.; Arianoutsou, M. How Effective Are the Protected Areas of the Natura 2000 Network in Halting Biological Invasions? A Case Study in Greece. *Plants* **2021**, *10*, 2113. [CrossRef]
43. López-Ballesteros, A.; Senent-Aparicio, J.; Martínez, C.; Pérez-Sánchez, J. Assessment of Future Hydrologic Alteration Due to Climate Change in the Aracthos River Basin (NW Greece). *Sci. Total Environ.* **2020**, *733*, 139299. [CrossRef] [PubMed]
44. Charalampopoulos, I.; Droulia, F. Frost Conditions Due to Climate Change in South-Eastern Europe via a High-Spatiotemporal-Resolution Dataset. *Atmosphere* **2022**, *13*, 1407. [CrossRef]
45. Kalfas, I.; Anagnostopoulou, C.; Manios, E.M. The Impact of Climate Change on Olive Crop Production in Halkidiki, Greece. *Environ. Sci. Proc.* **2023**, *26*, 69. [CrossRef]
46. Mavromatis, T. Crop–Climate Relationships of Cereals in Greece and the Impacts of Recent Climate Trends. *Theor. Appl. Climatol.* **2015**, *120*, 417–432. [CrossRef]
47. Stefanidis, S.; Alexandridis, V.; Chatzichristaki, C.; Stefanidis, P. Assessing Soil Loss by Water Erosion in a Typical Mediterranean Ecosystem of Northern Greece under Current and Future Rainfall Erosivity. *Water* **2021**, *13*, 2002. [CrossRef]
48. Kourgialas, N.N. A Critical Review of Water Resources in Greece: The Key Role of Agricultural Adaptation to Climate-Water Effects. *Sci. Total Environ.* **2021**, *775*, 145857. [CrossRef]
49. Koufos, G.; Mavromatis, T.; Koundouras, S.; Fyllas, N.M.; Jones, G.V. Viticulture-Climate Relationships in Greece: The Impacts of Recent Climate Trends on Harvest Date Variation. *Int. J. Climatol.* **2014**, *34*, 1445–1459. [CrossRef]
50. Lazoglou, G.; Anagnostopoulou, C.; Koundouras, S. Climate Change Projections for Greek Viticulture as Simulated by a Regional Climate Model. *Theor. Appl. Climatol.* **2018**, *133*, 551–567. [CrossRef]
51. Koufos, G.C.; Mavromatis, T.; Koundouras, S.; Jones, G.V. Adaptive Capacity of Winegrape Varieties Cultivated in Greece to Climate Change: Current Trends and Future Projections. *OENO One* **2020**, *54*, 1201–1219. [CrossRef]
52. Charalampopoulos, I. Agrometeorological Conditions and Agroclimatic Trends for the Maize and Wheat Crops in the Balkan Region. *Atmosphere* **2021**, *12*, 671. [CrossRef]
53. Georgilas, I.; Moulogianni, C.; Bournaris, T.; Vlontzos, G.; Manos, B. Socioeconomic Impact of Climate Change in Rural Areas of Greece Using a Multicriteria Decision-Making Model. *Agronomy* **2021**, *11*, 1779. [CrossRef]

54. Ullah, S.; You, Q.; Sachindra, D.A.; Nowosad, M.; Ullah, W.; Bhatti, A.S.; Jin, Z.; Ali, A. Spatiotemporal Changes in Global Aridity in Terms of Multiple Aridity Indices: An Assessment Based on the CRU Data. *Atmos. Res.* **2022**, *268*, 105998. [CrossRef]
55. Biasi, B.; Ferrara, C. Salvati Assessing Impacts of Climate Change on Phenology and Quality Traits of *Vitis Vinifera* L.: The Contribution of Local Knowledge. *Plants* **2019**, *8*, 121. [CrossRef]
56. Bucur, G.M.; Cojocaru, G.A.; Antoce, A.O. The Climate Change Influences and Trends on the Grapevine Growing in Southern Romania: A Long-Term Study. *BIO Web Conf.* **2019**, *15*, 01008. [CrossRef]
57. Mavrakis, A.; Kapsali, A.; Tsiros, I.X.; Pantavou, K. Air Quality and Meteorological Patterns of an Early Spring Heatwave Event in an Industrialized Area of Attica, Greece. *Euro-Mediterr. J. Environ. Integr.* **2021**, *6*, 25. [CrossRef] [PubMed]
58. Nastos, P.T.; Zerefos, C.S. Spatial and Temporal Variability of Consecutive Dry and Wet Days in Greece. *Atmos. Res.* **2009**, *94*, 616–628. [CrossRef]
59. Nastos, P.T.; Politi, N.; Kapsomenakis, J. Spatial and Temporal Variability of the Aridity Index in Greece. *Atmos. Res.* **2013**, *119*, 140–152. [CrossRef]
60. Founda, D.; Katavoutas, G.; Pierros, F.; Mihalopoulos, N. Centennial Changes in Heat Waves Characteristics in Athens (Greece) from Multiple Definitions Based on Climatic and Bioclimatic Indices. *Glob. Planet. Chang.* **2022**, *212*, 103807. [CrossRef]
61. Politi, N.; Vlachogiannis, D.; Sfetsos, A.; Nastos, P.T. High-Resolution Dynamical Downscaling of ERA-Interim Temperature and Precipitation Using WRF Model for Greece. *Clim. Dyn.* **2021**, *57*, 799–825. [CrossRef]
62. Tsiros, I.X.; Nastos, P.; Proutsos, N.D.; Tsaousidis, A. Variability of the Aridity Index and Related Drought Parameters in Greece Using Climatological Data over the Last Century (1900–1997). *Atmos. Res.* **2020**, *240*, 104914. [CrossRef]
63. Doxa, A.; Prastacos, P. Using Rao's Quadratic Entropy to Define Environmental Heterogeneity Priority Areas in the European Mediterranean Biome. *Biol. Conserv.* **2020**, *241*, 108366. [CrossRef]
64. Droulia, F.E.; Tsiros, I.X. The Outdoor Thermal Climate Conditions at a Historical Mountainous Tuberculosis Sanatorium Site in Greece. *Weather* **2019**, *74*, 221–225. [CrossRef]
65. Proutsos, N.; Tigkas, D. Growth Response of Endemic Black Pine Trees to Meteorological Variations and Drought Episodes in a Mediterranean Region. *Atmosphere* **2020**, *11*, 554. [CrossRef]
66. Guerra-Hernández, J.; Arellano-Pérez, S.; González-Ferreiro, E.; Pascual, A.; Sandoval Altelarrea, V.; Ruiz-González, A.D.; Álvarez-González, J.G. Developing a Site Index Model for P. Pinaster Stands in NW Spain by Combining Bi-Temporal ALS Data and Environmental Data. *For. Ecol. Manag.* **2021**, *481*, 118690. [CrossRef]
67. Tigkas, D.; Vangelis, H.; Tsakiris, G. Implementing Crop Evapotranspiration in RDI for Farm-Level Drought Evaluation and Adaptation under Climate Change Conditions. *Water Resour. Manag.* **2020**, *34*, 4329–4343. [CrossRef]
68. Pavlidis, V.; Kartsios, S.; Karypidou, M.C.; Katragkou, E. Future Evolution of Agroclimatic Indicators over a Viticulture Area in Greece. *Environ. Sci. Proc.* **2023**, *26*, 151. [CrossRef]
69. Charalampopoulos, I.; Polychroni, I.; Psomiadis, E.; Nastos, P. Spatiotemporal Estimation of the Olive and Vine Cultivations' Growing Degree Days in the Balkans Region. *Atmosphere* **2021**, *12*, 148. [CrossRef]
70. Ontel, I.; Vladut, A. Impact of Drought on the Productivity of Agricultural Crops within the Oltenia Plain, Romania. *Geogr. Pannonica* **2015**, *19*, 9–19. [CrossRef]
71. Baltas, E. Spatial distribution of climatic indices in northern Greece. *Meteorol. Appl.* **2007**, *14*, 69–78. [CrossRef]
72. Savo, V.; De Zuliani, E.; Salvati, L.; Perini, L.; Caneva, G. Long-Term Changes in Precipitation and Temperature Patterns and Their Possible Impacts on Vegetation (Tolfa–Cerite Area, Central Italy). *Appl. Ecol. Environ. Res.* **2012**, *10*, 243–266. [CrossRef]
73. Vessella, F.; Schirone, B. Forest Conservation and Restoration Using the Emberger Index: Cork Oak as Study Case. *Forests* **2022**, *13*, 252. [CrossRef]
74. Caloiero, T.; Callegari, G.; Cantasano, N.; Coletta, V.; Pellicone, G.; Veltri, A. Bioclimatic Analysis in a Region of Southern Italy (Calabria). *Plant Biosyst.—Int. J. Deal. All Asp. Plant Biol.* **2016**, *150*, 1282–1295. [CrossRef]
75. Gavilán, R.G. The Use of Climatic Parameters and Indices in Vegetation Distribution. A Case Study in the Spanish Sistema Central. *Int. J. Biometeorol.* **2005**, *50*, 111–120. [CrossRef]
76. Cutini, M.; Flavio, M.; Giuliana, B.; Guido, R.; Jean-Paul, T. Bioclimatic Pattern in a Mediterranean Mountain Area: Assessment from a Classification Approach on a Regional Scale. *Int. J. Biometeorol.* **2021**, *65*, 1085–1097. [CrossRef] [PubMed]
77. Eccel, E.; Zollo, A.L.; Mercogliano, P.; Zorer, R. Simulations of Quantitative Shift in Bio-Climatic Indices in the Viticultural Areas of Trentino (Italian Alps) by an Open Source R Package. *Comput. Electron. Agric.* **2016**, *127*, 92–100. [CrossRef]
78. Cao Pinna, L.; Axmanová, I.; Chytrý, M.; Malavasi, M.; Acosta, A.T.R.; Giulio, S.; Attorre, F.; Bergmeier, E.; Biurrun, I.; Campos, J.A.; et al. The Biogeography of Alien Plant Invasions in the Mediterranean Basin. *J. Veg. Sci.* **2021**, *32*, e12980. [CrossRef]
79. Reis, F.; Valdiviesso, T.; Varela, C.; Tavares, R.M.; Baptista, P.; Lino-Neto, T. Ectomycorrhizal Fungal Diversity and Community Structure Associated with Cork Oak in Different Landscapes. *Mycorrhiza* **2018**, *28*, 357–368. [CrossRef] [PubMed]
80. Schirone, B.; Radoglou, K.; Vessella, F. Conservation and Restoration Strategies to Preserve the Variability of Cork Oak *Quercus suber*—A Mediterranean Forest Species—Under Global Warming. *Clim. Res.* **2016**, *71*, 171–185. [CrossRef]
81. Gerassis, S.; Albuquerque, M.T.D.; Roque, N.; Ribeiro, S.; Taboada, J.; Ribeiro, M.M. Future Habitat Suitability for Species under Climate Change—Lessons Learned from the Strawberry Tree Case Study. *For. Ecol. Manag.* **2021**, *491*, 119150. [CrossRef]
82. López-Tirado, J.; Vessella, F.; Schirone, B.; Hidalgo, P.J. Trends in Evergreen Oak Suitability from Assembled Species Distribution Models: Assessing Climate Change in South-Western Europe. *New For.* **2018**, *49*, 471–487. [CrossRef]

83. Nikolova, N.; Yanakiev, D. Climate Aridity in Southern Bulgaria for the Period 1961–2015. In *Proceedings of the Forum Geografic*; Boengiu, S., Popescu, L., Eds.; University of Craiova, Department of Geography: Craiova, Romania, 2020; Volume 19, pp. 10–17.
84. García-Barrón, L.; Morales, J.; Sousa, A. Time Analysis of Emberger's Pluviothermic Q Index in the SW of the Iberian Peninsula. In *Proceedings of the Patterns and Mechanisms of Climate, Paleoclimate and Paleoenvironmental Changes from Low-Latitude Regions*; Zhang, Z., Khélifi, N., Mezghani, A., Heggy, E., Eds.; Springer International Publishing: Cham, Switzerland, 2019; pp. 45–47.
85. Koutsias, N.; Arianoutsou, M.; Kallimanis, A.S.; Mallinis, G.; Halley, J.M.; Dimopoulos, P. Where Did the Fires Burn in Peloponnisos, Greece the Summer of 2007? Evidence for a Synergy of Fuel and Weather. *Agric. For. Meteorol.* **2012**, *156*, 41–53. [CrossRef]
86. Mitsopoulos, I.; Xanthopoulos, G. Effect of Stand, Topographic, and Climatic Factors on the Fuel Complex Characteristics of Aleppo (*Pinus halepensis* Mill.) and Calabrian (*Pinus brutia* Ten.) Pine Forests of Greece. *For. Ecol. Manag.* **2016**, *360*, 110–121. [CrossRef]
87. Xystrakis, F.; Koutsias, N. Differences of Fire Activity and Their Underlying Factors among Vegetation Formations in Greece. *IFOREST* **2013**, *6*, 132–140. [CrossRef]
88. Brofas, G.; Karetsos, G.; Dimopoulos, P.; Tsagari, C. The Natural Environment of Cupressus Sempervirens in Greece as a Basis for Its Use in the Mediterranean Region. *Land Degrad. Dev.* **2006**, *17*, 645–659. [CrossRef]
89. Mela, F.; Ganatsas, P. Effect of Land Preparation Methods on Restoration Success of Degraded Oak Forest Ecosystems. *Dendrobiology* **2023**, *89*, 56–64. [CrossRef]
90. Hatzichristaki, C.; Zagas, T. The Contribution of Natural and Artificial Regeneration at the Restoration of Fire-Affected Peri-Urban Forest of Thessaloniki (Northern Greece). *Glob. Nest J.* **2017**, *19*, 29–36. [CrossRef]
91. Maloupa, E.; Krigas, N.; Grigoriadou, K.; Lazari, D.; Tsoktouridis, G. Conservation Strategies for Native Plant Species and Their Sustainable Exploitation: Case of the Balkan Botanic Garden of Kroussia, N Greece. *Floric. Ornam. Biotechnol.* **2008**, *5*, 37–56.
92. Baliousis, E.; Yannitsaros, A. Vascular Plant Diversity of Mt Pendelikon (Sterea Ellas, Greece): A Recent Inventory Reflecting Contemporary Dynamics. *Willdenowia* **2011**, *41*, 151–165. [CrossRef]
93. Baliousis, E. Flora and Vegetation of Mt Aphrodisio (Peloponnisos, Greece). *Fl. Medit.* **2016**, *26*, 31–61. [CrossRef]
94. Sarika, M.; Bazos, I.; Zervou, S.; Christopoulou, A. Flora and Vegetation of the European-Network "Natura 2000" Habitats of Naxos Island (GR4220014) and of Nearby Islets Mikres Kyklades (GR4220013), Central Aegean (Greece). *Plant Sociol.* **2015**, *52*, 3–56. [CrossRef]
95. Sarika, M.; Papanikolaou, A.; Yannitsaros, A.; Chitos, T.; Panitsa, M. Temporal Turnover of the Flora of Lake Islands: The Island of Lake Pamvotis (Epirus, Greece). *Biodivers. Data J.* **2019**, *7*, e37023. [CrossRef] [PubMed]
96. Gaitanis, A.; Kalogeropoulos, K.; Detsis, V.; Chalkias, C. Monitoring 60 Years of Land Cover Change in the Marathon Area, Greece. *Land* **2015**, *4*, 337–354. [CrossRef]
97. Tziritis, E.P. Environmental Monitoring of Micro Prespa Lake Basin (Western Macedonia, Greece): Hydrogeochemical Characteristics of Water Resources and Quality Trends. *Environ. Monit. Assess.* **2014**, *186*, 4553–4568. [CrossRef] [PubMed]
98. Fijani, E.; Barzegar, R.; Deo, R.; Tziritis, E.; Skordas, K. Design and Implementation of a Hybrid Model Based on Two-Layer Decomposition Method Coupled with Extreme Learning Machines to Support Real-Time Environmental Monitoring of Water Quality Parameters. *Sci. Total Environ.* **2019**, *648*, 839–853. [CrossRef] [PubMed]
99. Strid, A.; Tan, K. (Eds.) *Flora Hellenica*, 1st ed.; Lubrecht & Cramer Ltd.: Königstein, Germany, 1997; ISBN 978-3-87429-391-4.
100. Dimopoulos, P.; Raus, T.; Bergmeier, E.; Constantinidis, T.; Iatrou, G.; Kokkini, S.; Strid, A.; Tzanoudakis, D. *Vascular Plants of Greece: An Annotated Checklist*; Botanic Garden and Botanical Museum Berlin-Dahlem: Berlin, Germany, 2013; 372p.
101. Dimopoulos, P.; Raus, T.; Bergmeier, E.; Constantinidis, T.; Iatrou, G.; Kokkini, S.; Strid, A.; Tzanoudakis, D. Vascular Plants of Greece: An Annotated Checklist. Supplement. *Willdenowia* **2016**, *46*, 301–347. [CrossRef]
102. Dimopoulos, P.; Raus, T.; Strid, A. Flora of Greece Web. Vascular Plants of Greece: An Annotated Checklist. Version III. Available online: http://portal.cybertaxonomy.org/flora-greece (accessed on 15 April 2024).
103. Dimopoulos, P. Floristic Diversity of Greece: October 2013–July 2022. *Newsletter of the Hellenic Botanical Society*, 2022; Volume 11. Available online: https://www.hbs.gr/sites/default/files/newsletter/ebe-newsletter-11-012-hi.pdf (accessed on 29 June 2024).
104. Fick, S.E.; Hijmans, R.J. WorldClim 2: New 1-Km Spatial Resolution Climate Surfaces for Global Land Areas. *Int. J. Climatol.* **2017**, *37*, 4302–4315. [CrossRef]
105. Läderach, P.; Martinez-Valle, A.; Schroth, G.; Castro, N. Predicting the Future Climatic Suitability for Cocoa Farming of the World's Leading Producer Countries, Ghana and Côte d'Ivoire. *Clim. Chang.* **2013**, *119*, 841–854. [CrossRef]
106. Beck, J. Predicting Climate Change Effects on Agriculture from Ecological Niche Modeling: Who Profits, Who Loses? *Clim. Chang.* **2013**, *116*, 177–189. [CrossRef]
107. Panagos, P.; Borrelli, P.; Matthews, F.; Liakos, L.; Bezak, N.; Diodato, N.; Ballabio, C. Global Rainfall Erosivity Projections for 2050 and 2070. *J. Hydrol.* **2022**, *610*, 127865. [CrossRef]
108. Kass, J.M.; Guénard, B.; Dudley, K.L.; Jenkins, C.N.; Azuma, F.; Fisher, B.L.; Parr, C.L.; Gibb, H.; Longino, J.T.; Ward, P.S.; et al. The Global Distribution of Known and Undiscovered Ant Biodiversity. *Sci. Adv.* **2022**, *8*, eabp9908. [CrossRef] [PubMed]
109. Sanczuk, P.; De Pauw, K.; De Lombaerde, E.; Luoto, M.; Meeussen, C.; Govaert, S.; Vanneste, T.; Depauw, L.; Brunet, J.; Cousins, S.A.O.; et al. Microclimate and Forest Density Drive Plant Population Dynamics under Climate Change. *Nat. Clim. Chang.* **2023**, *13*, 840–847. [CrossRef]

110. Wen, S.; Wang, Y.; Tang, T.; Su, C.; Li, B.; Bilal, M.A.; Meng, Y. The Spatial-Temporal Patterns and Driving Mechanisms of the Ecological Barrier Transition Zone in the Western Jilin, China. *Land* **2024**, *13*, 856. [CrossRef]
111. Wan, Q.; Du, S.; Chen, Y.; Li, F.; Salah, R.; Njenga, M.N.; Li, J.; Wang, S. Ecological Niche Differentiation and Response to Climate Change of the African Endemic Family Myrothamnaceae. *Plants* **2024**, *13*, 1544. [CrossRef]
112. Cerasoli, F.; D'Alessandro, P.; Biondi, M. Worldclim 2.1 versus Worldclim 1.4: Climatic Niche and Grid Resolution Affect between-Version Mismatches in Habitat Suitability Models Predictions across Europe. *Ecol. Evol.* **2022**, *12*, e8430. [CrossRef]
113. Evans, J.S.; Murphy, M.A.; Ram, K. SpatialEco: Spatial Analysis and Modelling Utilities. Available online: https://CRAN.R-project.org/package=spatialEco (accessed on 12 December 2022).
114. Wickham, H. The Tidyverse. Available online: https://www.tidyverse.org/ (accessed on 15 April 2023).
115. Wickham, H.; François, R.; Henry, L.; Müller, K. Dplyr: A Grammar of Data Manipulation. Available online: https://CRAN.R-project.org/package=dplyr (accessed on 25 April 2020).
116. Wickham, H.; Chang, W.; Henry, L.; Pedersen, T.L.; Takahashi, K.; Wilke, C.; Woo, K.; Yutani, H.; Dunnington, D. Ggplot2: Create Elegant Data Visualisations Using the Grammar of Graphics. Available online: https://CRAN.R-project.org/package=ggplot2 (accessed on 5 February 2020).
117. Hijmans, R.J.; Bivand, R.; Forner, K.; Ooms, J.; Pebesma, E.; Sumner, M.D. Terra: Spatial Data Analysis. Available online: https://CRAN.R-project.org/package=terra (accessed on 7 July 2022).
118. Kougioumoutzis, K.; Kokkoris, I.P.; Strid, A.; Raus, T.; Dimopoulos, P. Climate-Change Impacts on the Southernmost Mediterranean Arctic-Alpine Plant Populations. *Sustainability* **2021**, *13*, 13778. [CrossRef]
119. Kougioumoutzis, K.; Papanikolaou, A.; Kokkoris, I.P.; Strid, A.; Dimopoulos, P.; Panitsa, M. Climate Change Impacts and Extinction Risk Assessment of Nepeta Representatives (Lamiaceae) in Greece. *Sustainability* **2022**, *14*, 4269. [CrossRef]
120. Grillakis, M.G.; Kapetanakis, E.G.; Goumenaki, E. Climate Change Implications for Olive Flowering in Crete, Greece: Projections Based on Historical Data. *Clim. Chang.* **2022**, *175*, 7. [CrossRef]
121. Kougioumoutzis, K.; Trigas, P.; Tsakiri, M.; Kokkoris, I.P.; Koumoutsou, E.; Dimopoulos, P.; Tzanoudakis, D.; Iatrou, G.; Panitsa, M. Climate and Land-Cover Change Impacts and Extinction Risk Assessment of Rare and Threatened Endemic Taxa of Chelmos-Vouraikos National Park (Peloponnese, Greece). *Plants* **2022**, *11*, 3548. [CrossRef]
122. Siebert, S.F. Traditional Agriculture and the Conservation of Biological Diversity in Crete, Greece. *Int. J. Agric. Sustain.* **2004**, *2*, 109–117. [CrossRef]
123. Petaloudi, L.-M.; Ganatsas, P.; Tsakaldimi, M. Exploring Biodiversity and Disturbances in the of Peri-Urban Forests of Thessaloniki, Greece. *Sustainability* **2022**, *14*, 8497. [CrossRef]
124. Spanou, S.; Tiniakou, A.; Georgiadis, T. Exploring Agroecosystem Floristic and Vegetation Diversity in a Mediterranean Landscape. *J. Biodivers. Environ. Sci. (JBES)* **2013**, *3*, 2220–6663.
125. Papaporfyriou, P.K.; Sarrou, E.; Avramidou, E.; Abraham, E.M. Abundance and Phenotypic Diversity of the Medicinal Sideritis Scardica Griseb. in Relation to Floristic Composition of Its Habitat in Northern Greece. *Sustainability* **2020**, *12*, 2542. [CrossRef]